UNIVERSITÉ DU QUÉBEC À MONTRÉAL

NOVEL GENES IMPLICATED IN THE DEVELOPMENT OF THE NERVOUS SYSTEM IN *C. ELEGANS*

MÉMOIRE

PRÉSENTÉ

COMME EXIGENCE PARTIELLE

DE LA MAÎTRISE EN BIOCHIMIE

PAR

VICTORIA CERDEIRA

SEPTEMBRE 2022

UNIVERSITÉ DU QUÉBEC À MONTRÉAL

NOUVEAUX GENES IMPLIQUÉS DANS LE DÉVELOPPEMENT NEURONAL CHEZ *C. ELEGANS*

MÉMOIRE

PRÉSENTÉ

COMME EXIGENCE PARTIELLE

DE LA MAÎTRISE EN BIOCHIMIE

PAR

VICTORIA CERDEIRA

SEPTEMBRE 2022

ACKNOWLEDGMENTS

First and foremost, I want to thank Claire Bénard. Since the day we met on Skype, half across the world, me in Argentina and her in Canada, she made me feel that I was cared for. Not only is she intelligent, wise, and an amazing scientist, but she is also an incredible person, with a gentle and caring soul. She offered her help from my first day as an intern at her lab back in 2018, all the way to the end of this Master's and I have no doubt she will continue helping me throughout all of my life stages. She taught me about *C. elegans*, project management, critical thinking, and all the important things a scientist needs to have. She also taught me incredibly valuable lessons about life, love, friendship, and leadership, among many other things. I don't have enough words to thank you for every conversation, motivational talk, understanding, helping, and taking care of me while being far away from home. I will be eternally grateful for having met you and being part of your lab. Las gracias infinitas se quedan cortas!

I want to thank all past and present Bénard Lab members, whom I was lucky to have met, helped, and laughed with. I want to particularly thank Lise Rivollet for all her support and advice. Your help was incredibly valuable while getting used to a new model organism, every time I was struggling with methods that wouldn't work, and every time I couldn't find the answers I was looking for. We are extremely lucky to have you in the lab! I also want to thank the two students who I was lucky to have working with me on this project, Myriam Ares and Cynthia Lanteigne. I had the opportunity to teach them about science, and their contributions were extremely important to this project. Not only did we learn science together, but they also taught me how to better communicate, and understand different points of view, giving me valuable leadership skills. I also loved being part of their learning, making their life decisions, and cherishing every step we made together. Thank you for being part of the project!

Importantly, I want to thank UQAM and the Biological Sciences Department for opening the doors of such an amazing environment. Although I arrived in Montreal knowing basic French, the staff received me with open arms, helped me improve my French, and understood my struggles. I was also honored to have received numerous scholarships from the CERMO-FC research center, the Biochemistry Program, the Faculty of Sciences, and the Fonds de Recherche en Sciences et Nature (FRQNT). For this, I want to say I am extremely thankful for the opportunities, for the mentions, and the financial and academic help each one of these scholarships has offered me. This kind of support and recognition were crucial in motivating and orienting my studies. Thank you for believing in me, in my professional and academic experience, and for trusting me with generating science knowledge.

I want to enormously thank every single teacher I met, either in the courses, in hallways, at conferences, or at seminars. I have always admired teachers and their incredible mission of transmitting knowledge to students. As students, we will always be thankful to have teachers that offer us knowledge, advice, and that also help us become better scientists and persons. I want to particularly thank Benoît Barbeau and Marc Lussier for being the judges of this thesis. I know this was an “out of the blue” assignment to add to your busy schedules, so I really appreciate the time you took to evaluate this thesis. Not only were you extremely important for this thesis, but I am also incredibly thankful to have had meaningful conversations with each one of you. Thank you for your advice, your knowledge, and your help.

Of course, I couldn’t have done any of this without “my people”. My people half around the world in that amazing country down south. To all of my Argentinean friends, my scientist group, and my not-at-all scientist group. This is the second thesis I add you to in my acknowledgment sections, which means that you are extremely important to me. To my favorite scientist group, Dani, Naty, Cata, Fran, Pau, Maru, Tincho, thank you for supporting me through my ups and my downs. Thank you for sharing and understanding the struggle that one goes through in science research, with

failed experiments, thinking about our undefined future, and the emotional rollercoaster all of this is. Thank you for still being present although I am half away the world and thank you for reaching out every time I said I needed advice. As for my first thesis, and now the second one, I am certain I couldn't have done all of this without you. Los adoro con el alma, chiquis! And to my not-at-all scientist group, my two best friends, Bel and Tama, who I met back then in sign language course, and have become forever life-long friends. You are my emotional support, my constant reminder of self-awareness and comfort. Through really high ups and really low downs, you always find a way of making me talk, even when I can't find the words to express my feelings. Thank you for making me understand that I am worthy, that I am loved, and that I am cared for. Saben que las amo con el alma entera!

The other part of "my people" are the ones I started making at my new home, here in Montreal. I have met a lot of amazing people, both inside and outside of the lab. But I want to particularly thank two people. The first one is my Montrealer best friend, Eleni, who I met dancing salsa and since then we have been inseparable. Thank you for all your love, your advice, your beautiful craziness, and our adventures. Thank you for coaching me as well, I learned a lot with the hours and hours of conversations we have every time we meet. Te adoro mi querida Griega con alma Latina!

And last, but definitely not least, is my favorite Montrealer/Martinican person I have in my life. Dancing salsa in a non-latino country has a way of bringing people together, and this is how I met Xavier. Your love and support made me understand that I was never asking for too much, I was just asking it to the wrong people. With you, I've learned what it is to just stop and feel. You made me realize a lot of things about myself, my triggers, and my past trauma. But above all, you gave me the space to slowly process it, with an infinite amount of hugs and undeniable support. I could go on and on about how you changed my life, but you already know. I thank you from the bottom of my heart for all your love, your support, your words of motivation, and every single

thing you have done for me in these last 2 years and a half. Te amo, mi Loquito, mañamaña!

Finally, I want to thank my Grandmother, Abuela Mary. She is a source of inspiration and strength. You took care of me since I was very young, like a second mother. Your love and support have been vital for all my accomplishments. I will never get tired of thanking you for everything you did for me, every single hug, message, and act of love. Te amo hoy y siempre!

This work was supported with scholarships to Victoria Cerdeira from the Faculty of Sciences at UQAM, scholarships from the CERMO-FC Research Center, and scholarships from the Fonds de Recherche en Sciences et Nature (FRQNT). Several grants of the Bénard laboratory funded this research project, including from Natural Sciences and Engineering Research Council of Canada (NSERC), Canadian Institutes of Health Research (CIHR), and Fonds de Recherche en Santé (FRQS), as well as from the National Institutes of Health (NIH) and National Science Foundation (NSF) (USA).

DEDICATION

A mi Ángel de la Guarda:

Sigo tu luz.

Confío en tu energía.

Seguí guiándome y poniéndome gente en el camino.

Gracias por lo que fuiste y lo que seguís siendo.

Te amo hoy y para siempre.

Released from my hands,

Forever sealed in my heart.

TABLE OF CONTENTS

LIST OF FIGURES

LIST OF TABLES

Table Page

LIST OF ABBREVIATIONS

bp	base pairs
C. elegans	*Caenorhabditis elegans*
cDNA	Complementary Deoxyribonucleic Acid
DNA	Deoxyribonucleic Acid
E. coli OP50	*Escherichia coli* OP50 strain
EMS	Ethyl Methane Sulfonate
F2-F3	reproductive generation 2-3
Fwd	Forward
GABA	γ-aminobutyric acid
GFP	Green Fluorescent Protein
L1-L4	Larval stages 1 to 4
M9	Medium 9
mRNA	messenger Ribonucleic Acid
NGM	Nematode Growth Media
p [lowercase]	plasmid
P [uppercase]	Promoter
P0	Progenitor generation
PCR	Polymerase Chain Reaction
Rev	Reverse
RNA	Ribonucleic Acid
rpm	revolutions per minute
UTR	Untranslated Regions
WT	wild-type worm
YAC	Yeast Artificial Chromosome

LIST OF SYMBOLS AND UNITS

°C	degrees Celsius
µL	microlitre
mm	millimeter
h	hour
min	minute
n.s	non-significant
~	approximately
mM	millimolar
%	percentage
s, sec	seconds

RÉSUMÉ

Le développement du système nerveux est un ensemble d'événements régulés et coordonnés basés sur des mécanismes moléculaires qui permettent la reconnaissance de signaux externes et internes, favorisant la croissance des neurones vers leur cible finale. La perturbation de certains de ces mécanismes peut entraîner des défauts dans le développement du système nerveux. Dans ce travail, nous étudions de mutants à locomotion non coordonnée qui ont été obtenus lors d'un criblage génétique à la recherche de mutations à effet maternel. Ces mutants présentent des phénotypes de locomotion sévèrement désordonnée, tels que la paralysie du corps, l'adoption de positions repliées et des mouvement anormaux. Nous avons caractérisé ces mutants par des essais de locomotion, par l'analyse de leurs réponses pharmacologiques, puis par l'examen de leur neuroanatomie. L'une des principales constatations est que ces mutants présentent des défauts de guidage axonal des neurones GABAergiques et cholinergiques, à la ligne médiane ventrale, ainsi que sur les aspects latéraux du corps des animaux. Pour identifier de manière moléculaire les gènes responsables de ces défauts de développement neuronal, des efforts antérieurs de séquençage du génome entier ont permis de trouver des mutations causales candidates, pour lesquelles les gènes correspondants ont été testés dans des essais de sauvetage. Certains essais de sauvetage réussis ont été obtenus, montrant un retour de la locomotion et de la croissance générale au type sauvage, ainsi qu'un sauvetage neuroanatomique des défauts pour l'un des mutants. Ces études sont un pas vers la découverte de nouveaux gènes impliqués dans le développement du système nerveux. Grâce à la conservation évolutive des gènes entre les humains et *C. elegans*, ce travail contribue à offrir de nouvelles perspectives sur les mécanismes moléculaires du développement neuronal et potentiellement améliorer notre compréhension des bases moléculaires de certains troubles neurodéveloppementaux chez l'humain.

Mots clés : *C. elegans*, développement, guidage axonal, mutations, système nerveux.

ABSTRACT

The development of the nervous system is a well-regulated and coordinated set of events based on molecular mechanisms that allow the recognition of external and internal cues, promoting the growth of neurons towards their final target. Disruption of these mechanisms can lead to defects in the development of the nervous system. In this work, we study a series of uncoordinated mutants that were obtained in a forward genetic screen looking for maternal-effect mutations. These mutants are severely uncoordinated, showing body paralysis, kinked bodies, and abnormal movements. Interestingly, since they are maternal-effect mutations, these worms only show defects in the second homozygous generation. Here, we characterized these mutants with locomotion assays, pharmacological assays, and examined aspects of their neuroanatomy. A key finding is that these mutants display GABAergic and cholinergic neurons midline and lateral axon guidance defects. To molecularly identify the genes responsible for these neurodevelopmental defects, prior whole-genome sequencing efforts had yielded candidate causal mutations, for which the corresponding genes were tested in rescue assays. Some successful rescue assays were obtained showing locomotion and overall growth back to wild type, as well as neuroanatomy rescue of defects for one of the mutants. These studies contribute to the discovery and analysis of novel genes implicated in neuronal development. Thanks to the significant homology of genes between humans and *C. elegans*, this work helps offer new insights into the molecular mechanisms of neuronal development and potentially further our understanding of the molecular bases of some human neurodevelopmental disorders.

Keywords: axon guidance, *C. elegans*, development, mutations, nervous system.

CHAPTER I

INTRODUCTION

Understanding the development of the nervous system has been a continued aim for countless neuroscientists. One of their motivations is to unravel the mysteries of organizing an organ as complex as the brain. Another motivation is their aspiration to uncover important mechanisms that could help find potential treatments for neurodevelopmental diseases. More complex organisms, like mice, are commonly used for this research, as are human cells, tissue explants, organoids, and induced pluripotent stem cells. However, neurons and synapses are very numerous and variable among individuals in mammals, making it much more difficult and limiting to finely dissect neurodevelopmental molecular mechanisms. Since 1974, Sydney Brenner has put *Caenorhabditis elegans*, a 1 mm nematode, in the spotlight for advanced studies of cellular and molecular mechanisms, particularly of the nervous system. Following Brenner's legacy, this project has aimed to characterize novel *C. elegans* mutants, with the goal of identifying additional genes implicated in the development of the nervous system.

1.1 Using *C. elegans* as a model organism

1.1.1 Characteristics of *C. elegans*

C. elegans was presented, 60 years ago by Sydney Brenner, as a biological model for understanding fundamental questions in neurobiology and developmental biology. The lack of model organisms that could allow extensive genetic studies, cell lineage tracing and the possibility of determining the complete structure of the nervous system was an intriguing point of entry to start studying *C. elegans* (Brenner, 1974). Thanks to his

pioneering work, the use of *C. elegans* as a model organism was propelled (Brenner, 1974). Extensive scientific advanced like the first complete characterization of the celllineage of a developing metazoan (1983), the discovery of apoptosis, and the subsequent identification of genes implicated in its regulation (1983, Nobel Prize 2002), the use of the green fluorescent protein GFP as a gene expression marker (1994, Nobel Prize 2008), the complete sequencing of a metazoan genome (1998), the entire mapping of a complete nervous system connectome, and the discovery of RNA interference and its characterization (1998, Nobel Prize 2006) (Chalfie et al., 1994; Consortium, 1998; Kelly & Fire, 1998; Sulston et al., 1983)

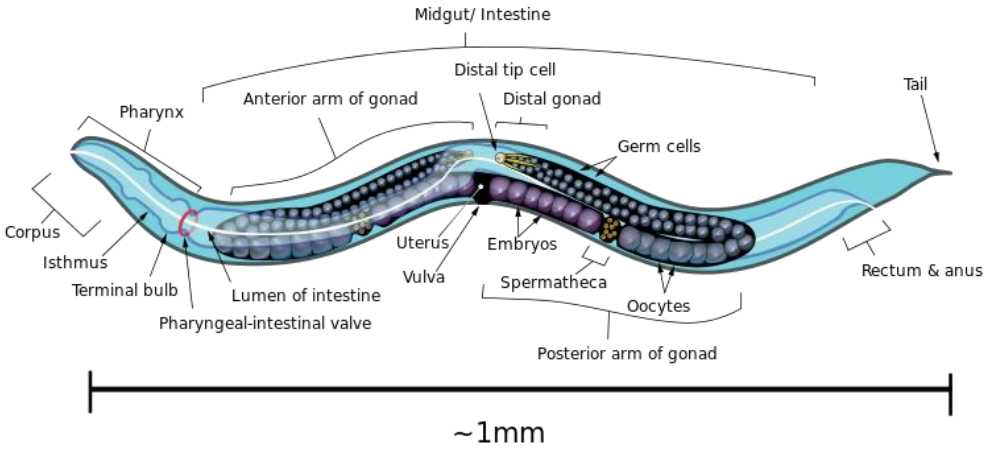

Figure 1.1: Schematic of an adult *C. elegans* hermaphrodite, showing distinct parts of the body. Image obtained from Microscope World.

C. elegans is a nematode that lives mainly in organic soils, on fruits and stems of rotting plants; thus, they can be easily isolated from there, its general structure can be seen in Figure 1.1. Its size oscillates from 0.25 mm for newly hatched larvae (L1 stage) up to 1 mm long for adults. Its life cycle is fast, transitioning from an embryo to an egg-laying adult in 3 days at 25°C. Regarding reproduction, *C. elegans* has two sexual forms: self-fertilizing hermaphrodites and males (Brenner, 1974). The hermaphrodites

produce sperm temporarily (at L4), and then produce uniquely oocytes, generating about 300 self-fertilized eggs. A juvenile hermaphrodite can accumulate 10-15 eggs in the uterus and expels 1 or 2 eggs at each opening of the vulva. This reproductive stage lasts 2-3 days until all the sperm stored in the spermatheca is consumed. This self-fertilization of hermaphrodites simplifies the maintenance of stocks since a single animal gives rise to a large, genetically identical population. However, mating with males is possible, and in that case, they can lay ~1000 eggs. Both sexes possess five identical diploid autosomal chromosomes and differ in the sex chromosomes: the hermaphrodite has two sex chromosomes (XX), while males have a single-sex chromosome X (X0). Most of the offspring produced by self-fertilization are hermaphrodites, and only 0.1-0.2 % of the progeny are male (Corsi et al., 2015).

C. elegans' embryogenesis takes about 14-16 hours (Figure 1.2). During this time, the first stages take place in-utero (until the 24-cell stage), followed by an ex-utero stage until the embryo hatches, transforming into larva 1 (L1). In the presence of food, the worm's normal development consists of 4 larval stages (L1-L4) defined by a series of pauses (i.e. molting, forming a new cuticle in each stage) and then reaches adulthood (Figure 1.2). The animals can live for approximately 3-4 weeks under suitable feeding and temperature conditions (Corsi et al., 2015). However, if food is absent during the L1 stage, the worm will undergo a series of changes and merge into an alternative life stage called "dauer". This stage is characterized by generating an ultra-resistant worm with a cuticle that covers the mouth, enhancing the protection of the body under the stressful environment and thus arresting its development. This cuticle has enhanced resistance to desiccation and chemicals, which decreases the susceptibility of the worm to other potential environmental stressors. Dauer larvae can survive for many months, and this is how they are commonly found in nature. Once the food is readily available again, the dauer larva will uncover its mouth, start eating and re-enter development into the L4 stage.

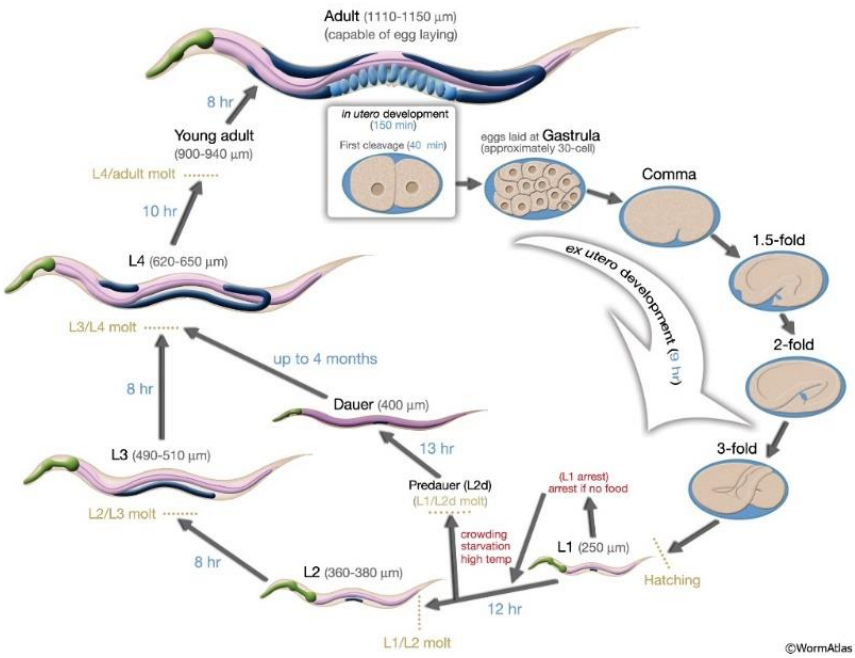

Figure 1.2: Schematic of the life cycle of *C. elegans* hermaphrodite at 22°C. The fertilization of the oocyte starts thanks to the passage through the spermatheca, initiating development. The embryo will then develop in-utero for 150 min, until it is laid. Outside of the uterus, embryogenesis continues for around 9 hours, until hatching, where the young larva (L1) is born. With available food and good conditions, the larva will pass through 4 larval stages (L1-L4). The morphogenesis of the vulva begins at the L3 stage and continues until L4, marking the maturation of the sexual organs. After this stage, the production of oocytes starts, entering the adult egg-laying stage. If unfavorable growing conditions are presented, ultra-resistant dauer worms are formed which will be able to resist hostile conditions. This condition is exited when food is readily available, continuing development to L4. Gray arrows: passage to another stage of development, the duration is indicated in light blue. Larva and hermaphrodite adult: pharynx (green), intestine (pink), gonad (dark blue), embryos (light blue). Image adapted from WormAtlas.

C. elegans was the first multicellular eukaryotic organism with its entire genome sequenced in 1998 (Consortium, 1998). Its genome is 100 Mb and has 20,444 protein-coding genes. Most of *C. elegans'* genes have an average size of 3 kb interrupted by relatively small introns, compared to vertebrate genes. Some interesting facts about the worm's genome are 1) most protein-coding mRNAs are trans-spliced (additional 22 nt

leader sequence, SL1 or SL2, at the 5’ end); and 2) some genes are organized in operons. Importantly, 60 to 80% of its genes have a human homolog potentially allowing the extrapolation of many mechanisms that are shared and conserved with humans during evolution.

1.1.2 The Nervous System in *C. elegans*

Most of the model organisms used in research, like flies and mice, have a vast number of neurons and synapses, embedded in high-complexity nervous systems, which make it difficult to fully understand the structure, function, intrinsic molecular mechanisms, and regulations of it, particularly at a single-neuron resolution. Luckily, Sydney Brenner’s suggestion of using the nematode as a model organism solved the problem. The worm is not only suitable for genetical studies but is also simple enough to determine the complete structure of the nervous system (Brenner, 1974).

Indeed, to study neurobiological questions, *C. elegans* is powerful and very well adapted. Vast research studies have elucidated mechanisms and genes needed for the specification of neurons, precursor migration, axon guidance, synapse formation, and neuronal function (like synaptic release during the control of chemosensory or mechanosensory transduction), all the way to the processes of neuronal degeneration, cell death, neurite regeneration, and implications of glial function (Hammarlund & Jin, 2014; Shaham, 2015). In addition, *C. elegans* has also been used to study both simple and complex behaviors such as chemosensation, feeding, egg-laying, aggregation and social attachment, and male mating (Bargmann, 2006; Barr & Garcia, 2006; Cheung et al., 2004; De Bono, 2003; Gray et al., 2004; Hart, 2006). Also, *C. elegans* has been used to study the neuronal basis of sleep, since it undergoes periods of restful inactivity (Raizen et al., 2008).

Mechanistic insights, as well as an understanding of the development and function of the nervous system in all animals, have been accomplished by extensive research with *C. elegans* (Brenner, 1974; Hedgecock et al., 1990). These insights were key

to advancing research in other systems. For instance, several of the key molecules known to be required for the guidance of axonal migrations during the development of nervous systems were first identified in *C. elegans* (e.g., *unc-6*/Netrin) (Hedgecock et al., 1990), and were later found to be conserved in vertebrates with similar functions. Also, numerous synaptic transmission components have been identified and defined by *C. elegans* research, which helped fuel advances in vertebrate systems (e.g., *unc-13*/Munc13 and *unc-18*/Munc18 synaptic components) (Brenner, 1974; Kohn et al., 2000; Sassa et al., 1999).

The increased complexity of the human nervous system (with 100 billion neurons) and variability among individuals, make it extremely difficult to elucidate molecular mechanisms linked to the development of the nervous system. In contrast, the highly invariant nervous system of *C. elegans'* adult hermaphrodite has exactly 302 neurons, and the male has 383 neurons (extra neurons are implicated in sexual reproduction) (Figure 1.3). These neurons are named with two to three capital letters which mostly do not represent an acronym (like DD, VD, DVB, among many others). However, some other names, do correspond to a specific name, for example HSN which stands for Hermaphrodite Specific Neuron. Most of the *C. elegans'* adult nervous system (~75%) develops during embryogenesis, with main stages related to the birth of neurons, cell migration, neurite extension, axonal guidance, reaching the final target and undergoing synaptogenesis, thus building the embryonic neuronal circuits. Once initial development is finished, 80 motor neurons are subsequently added during the first larval stage, mainly to the ventral nerve cord. Each neuron has unique properties, such as position, morphology, and connections, allowing the identification of individual neurons (White et al., 1986). Compared to the other anatomical systems of the worm's body, the nervous system of *C. elegans* represents the most complex tissue both in number (302 neurons and 56 glial cells) and in diversity (118 morphologically distinct classes) (Oliver Hobert, 2010). This makes *C. elegans'* nervous system an incredible

tool to study numerous scientific questions related to neurodevelopmental and neurodegenerative diseases.

C. elegans' nervous system has three main coordinating centers that localize most of the synapses: these are the nerve ring, and the ventral and dorsal nerve cords (Figure 1.3). The neuronal structure is quite simple, with one or two neurites exiting from the cell body, except for some sensory neurons that have branched neurites. Compared to higher complexity eukaryotes, nerve conduction in the worm was believed to be primarily passive, although recent studies have shown the presence of action potentials in specific neurons (Chen et al., 2020; Liu et al., 2018; Mellem et al., 2008). Neurons in *C. elegans* do not possess various axonal terminals with synaptic buttons to make synapses. Instead, axons are not myelinated and thus, most of the chemical and electrical connections are made *en passant*, allowing contact between neurites (Corsi et al., 2015). Regarding the synaptic complexity, as a reference, a mammalian pyramidal cell in the cortex possesses at least 10,000 synapses, whereas in *C. elegans* there are nearly 7,000 chemical synapses and junctional connections in total for the entire connectome (White et al., 1986).

The presence of 56 glial cells in *C. elegans*, although less numerous than in vertebrates, still offer important support and are mainly associated with sensory neurons (Oikonomou & Shaham, 2011). Like the mammalian nervous system, *C. elegans* uses neurotransmitters, including acetylcholine, glutamate, γ-aminobutyric acid (GABA), dopamine, and serotonin, and has several conserved receptors for their detection (O Hobert, 2013). Another source of neuronal regulation resides in neuroendocrine signals with different neuropeptides maintaining neuronal circuits (C. Li & Kim, 2008). Thus, *C. elegans* is an incredible molecular tool to understand how the nervous system is developed and regulated, thanks to the availability of information as well as the simplicity of its nervous system. This makes it ideal to study mechanisms involved in its development, function, and regulation.

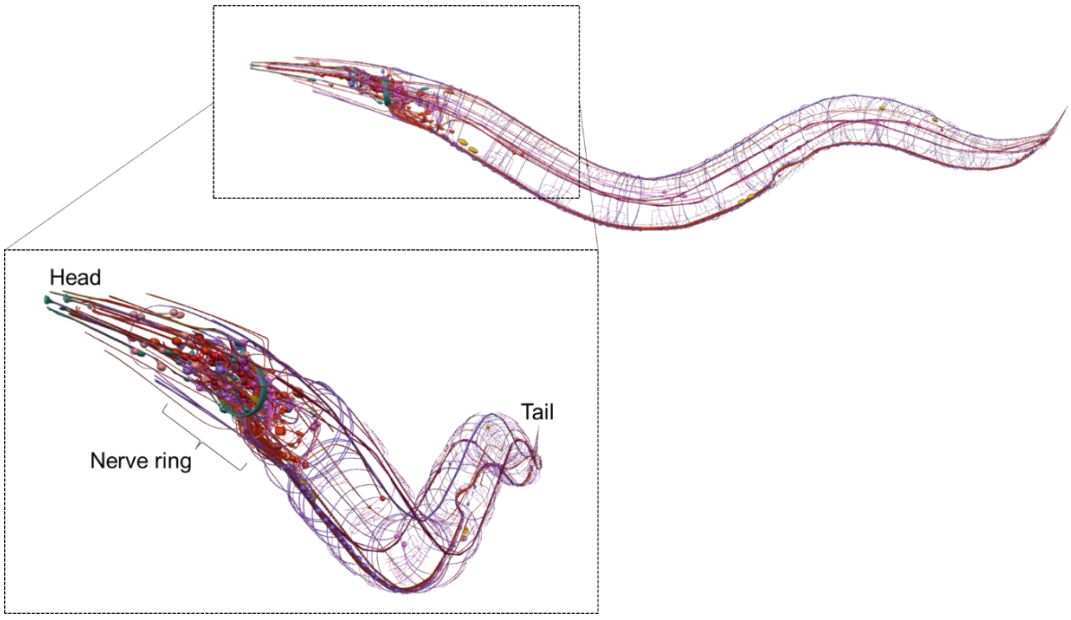

Figure 1.3: Schematic of the *C. elegans* nervous system. Colored lines and circles represent independent neurons throughout the body. The whole body of the worm is represented. The dotted square highlights the head of the worm to show more clearly the position of the nerve ring in the head and the significant number of neuronal bodies that exit it. Image adapted from Open Worm Browser and WormAtlas.

Another particularity of the worm is the transparency of its body. This allows detailed observation of live animals at any stage of their lives using fluorescence microscopy. In addition, scientists completely reconstructed the entire nervous system of the adult hermaphrodite with electron microscopy resolution back in 1986 (White et al., 1986), following the characterization of the male connectome (Cook et al., 2019) and more recently, hermaphrodites of different larval stages and other adults (Mulcahy et al., 2022; Witvliet et al., 2020). The community developed many approaches and techniques, generating extensive knowledge, and increasingly useful for studying biology. In particular, a large collection of mutant strains of neuronal development and synaptic transmission pathways, as well as numerous precise markers for individual cells or subcellular components (e.g., cytoskeleton, plasma membrane, mitochondria, synapses) are available and readily shared within the *C. elegans* community.

1.1.3 Neuronal guidance in *C. elegans*

The development of the nervous system is based initially on ectodermal neural precursors for the establishment of the neuronal population (Figure 1.4). With the absence of transcription factors or even cell death, the daughter cells of neuroblasts adopt distinct sizes and fates. Cell death is a major process, given that from 1090 somatic cells, 131 cells will die before differentiating, most of which belong to the ectodermal lineage (Rapti, 2020; Sulston et al., 1983). The complexity of the nervous system is defined by how diverse it is, accomplished by modifying the fates of daughter cells after neuroblast division. This is performed by generating intrinsic patterns along the axis of the body and the determination of the neuronal subtype. Throughout all these changes, transcription factors are essential to promote left-right orientation (leading to asymmetry) and the regulation of the final differentiation of neurons into subclasses (i.e. motorneuron, interneuron or sensory neurons) (Figure 1.4).

Next, neurons and their neurites migrate during development. Like in vertebrates, the growth cone is the primary navigation center in neurons in the worm, allowing for the recognition of external cues for correct neuronal oriented growth. Further, by modulating the cytoskeleton, these signals are integrated. A series of consecutive steps take place during the development and guidance of neurons. As part of the neuron's polarization process, the neurons must first recognize their parts, including their axons and dendrites. A series of cues will then guide the axon or dendrite to its target. Generally, axons travel longer distances, whereas dendrites cover a larger area near the cell's body and are mainly branched. After defining synaptic partners, pre- and post-synaptic neurons must coordinate synapse formation (Figure 1.4).

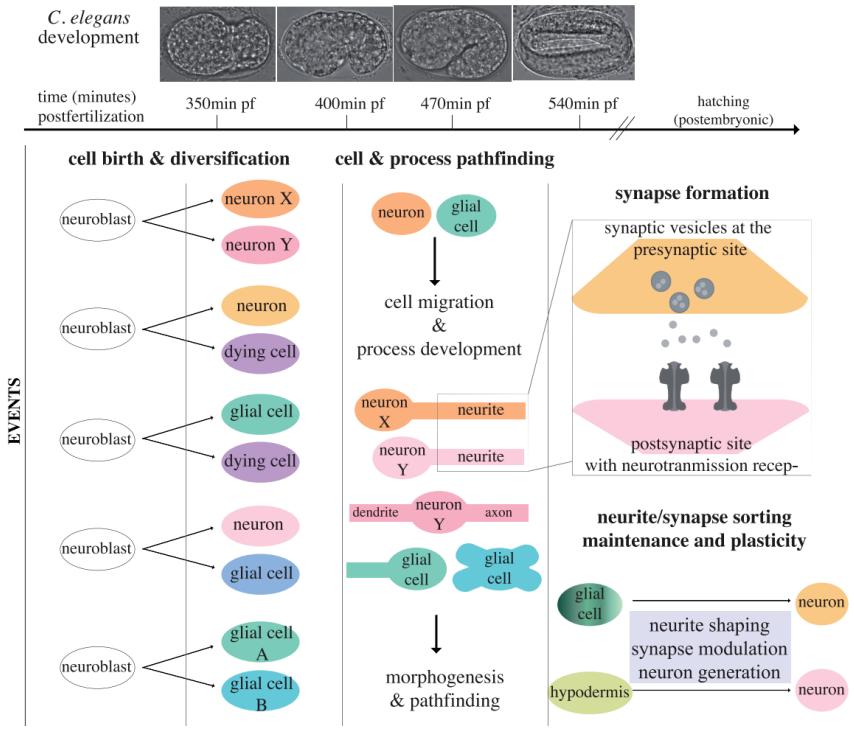

Figure 1.4: Neuronal development in *C. elegans* is orchestrated in several phases: neuronal birth, fate acquisition, neurite extension and synaptogenesis. Starting with neuroblasts that give rise to nervous system components (from left to right). Neurons and glia will migrate, grow, and diversify processes, finally reaching their targets and generating synaptic connections. Connections will be maintained by mechanisms acting in neuronal or glia and hypodermal cells. These last non-neuronal cells can generate post-embryonic neurons by division or differentiation, and in other cases, they can function in synapse maintenance or plasticity. Figure adapted from Rapti 2020.

Due to extensive studies done in *C. elegans* regarding the development and guidance of the nervous system, we know that three main conserved genes, namely *unc-5*, *unc-6*, and *unc-40*, control the directionality of circumferential cell migration and axon guidance (Hedgecock et al., 1990). Briefly, UNC-6/Netrin is secreted into the basement membrane along the ventral aspect of the animal and plays a key role in the guidance of axons dorsally and ventrally. In ventral cells, UNC-6 is produced and released; axons possess the receptor UNC-40 and are attracted to UNC-6, allowing growth toward the ventral nerve cord. However, axons expressing UNC-5, either alone or in conjunction

with UNC-40, will grow dorsally because UNC-6 repels them. Commissural (circumferential) motor neurons have the most extensive growth cones in the worm (Chisholm et al., 2016).

Neuronal guidance starts as the growth cone crosses through the ectoderm, forming longitudinal and circumferential tracts. However, some axons cross the midline to make connections on the opposite side. As soon as these initial migrations have occurred, later axons are likely to fasciculate with other established axons. The process of axonal guidance has been extensively studied, leading to a series of possible models of how it occurs.

A prevailing model suggests that growth cones respond to either chemoattractive or chemorepellent cues. In this model, the growth cone responds to signals associated with intermediate or final targets, directing outgrowth towards or away from target cells. The attraction-repulsion model suggests that axons can switch their responses at specific points based on external cues. This model also considers that the neuron's outgrowth movement results from a force produced by the neuronal cell in response to external cues at the plasma membrane.

In a second model, directed outgrowth is predicted to occur by a self-organizing mechanism that is responsible for bringing the necessary machinery to the surface of the neuron. Hence, the direction of outgrowth can be defined stochastically, allowing the site of outgrowth to be defined without external cues (Chisholm et al., 2016). This last model was proposed due to existing genetic information that conformational changes in the UNC-40 receptor can trigger independent signals (Chisholm et al., 2016).

As cells extend their axons, proteins need to be secreted or found in the extracellular environment to enable this outgrowth. These proteins can be classified into 1) basement membrane proteins (mainly collagen IV and laminin); 2) integrin receptors (*ina-1* and *pat-2*); 3) heparan sulfate proteoglycans (extracellular or membrane-bound proteins

with modified sugar chains); 4) tropic guidance cues (attractants or repellents); 5) receptors and adhesion molecules (mainly cadherins and the immunoglobulin family cell adhesion molecules).

Null allele mutants of axon guidance genes are not completely penetrant, suggesting that axon guidance is regulated redundantly. Likewise, mutations have had different effects and penetrance on different types of neurons, illustrating the cell-specific and context-dependency of these guidance mechanisms. For example, D-type motor neurons typically show more penetrant defects in guidance of commissures compared to motor neurons DA and DB (Chisholm et al., 2016).

Once neurons have followed guidance cues and reached their final targets, a phase of functional maturation and establishment neural connectivity starts. This requires protein localization to specific cellular compartments. As a result, neurites can compartmentalize and polarize with finely tuned anterograde and retrograde transport systems (Rapti, 2020). The process of synaptogenesis consists of the formation of a site for neurotransmitter release in the presynaptic neuron and its receptor in the postsynaptic neuron. Synapses in *C. elegans* have very distinct morphologies. Typically, the presynaptic terminal is surrounded by synaptic vesicles, while the postsynaptic terminal consists of ion channels and signal transduction molecules. The process begins with the formation of the presynaptic membrane. A presynaptic region can be formed at the membrane adjacent to the postsynaptic cell. In addition, synaptic vessels cluster around the region, and the active zone can be established (Rapti, 2020). The final step for functional connectivity, termed synaptogenesis, is defined by neurotransmitter release in a specialized localization and the following activity of the receptors for that neurotransmitter.

All the process of guidance of neuronal migrations, including axon guidance, neurite development, and synaptogenesis allows the formation of a well-structured and functional nervous system, where all neurons are connected to their targets and can

fulfill the regulation of molecular mechanisms implicated in responding to stimuli to drive behavior.

1.2 Neurons of interest for the studies presented here

1.2.1 GABAergic motor neurons

Among all the great discoveries using *C. elegans* as a model organism, the vesicular GABA transporter (VGAT) was first discovered in this organism (Gendrel et al., 2016; Mclntire et al., 1993), which then promoted the identification of the mammalian homolog. Briefly, mutations that disrupted GABA-mediated behaviors allowed to define proteins required for GABA function (Schuske et al., 2004). This revealed that 26 out of the 302 neurons express the neurotransmitter GABA (Figure 1.5). These neurons in *C. elegans* are 6 so-called DD neurons, 13 so-called VD neurons, 4 so-called RME neurons, 1 RIS neuron, 1 AVL neuron, and 1 DVB neuron (these neuron names do not correspond to acronyms and are simply part of the *C. elegans* neuronal nomenclature). The D-type neurons (DD and VD) are motor neurons that are essential for the sinusoidal movement of the body. The RME neurons are suggested to be the pioneers of the nerve ring. The RIS is an interneuron, and its function is not clearly known. Finally, AVL and DVB are polymodal neurons, since they act as a motor neuron and as an interneuron, and their principal function is being implicated in defecation. These neurons, at the same time, can be classified into different groups based on their synaptic outputs. For example, D-type neurons (DD and VD motor neurons) innervate the dorsal and ventral body muscles, respectively. The RME motor neuron innervates the head muscles; and the AVL and DVB motor neurons innervate the enteric muscles.

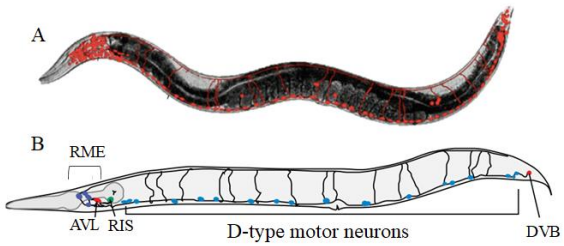

Figure 1.5: GABAergic nervous system in *C. elegans*. (A) Fluorescent schematic showing the 26 GABA neurons, labeled using an *unc-47p::mCherry* fluorescent marker (b) Schematic drawing of the positions of the 26 GABA neurons. Figure adapted from Schuske et al., 2004.

One interesting aspect of DD neurons is their ability to remodel their synapses during development (Figure 1.6). In the L1 larval stage, their synapses are innervating the muscles through their ventral neurites, receiving synaptic inputs from cholinergic neurons that are innervating dorsally. By adulthood, DD neurons will remodel their synapses and completely switch their connectivity. They eliminate synapses along their ventral neurites and reform synapses along their dorsal neurites. Although the VD neurons are born post-embryonically, share similar axon morphology as DD neurons, and innervate the ventral muscle, they do not undergo remodeling (Cuentas-condori & Miller, 2020).

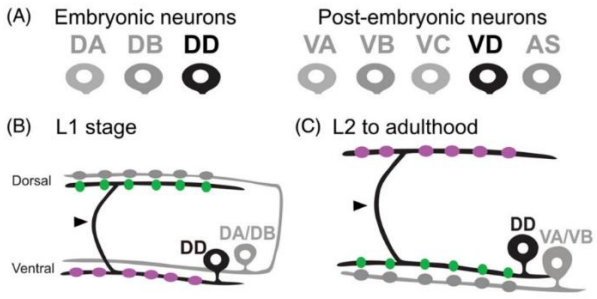

Figure 1.6: DD GABAergic neurons and their synaptic remodeling. Schematic of this remodeling in the early stages of development. (A) three classes of neurons are developed embryonically DA, DB, and DD. Some other motor neurons are developed post-embryonically (VA, VB, VC, VD, AS). (B) during the L1 stage, DD motor neurons innervate on body muscles on the ventral side and receive input

from cholinergic DA/DB neurons. (C) towards adulthood, DD neurons change their presynaptic terminals to the dorsal side, and their postsynaptic terminals to the ventral side, receiving input from VA/VB cholinergic motor neurons. Figure adapted from Cuentas-Condori et al., 2020.

1.2.2 Cholinergic motor neurons

As in most animals, acetylcholine is an essential neurotransmitter in *C. elegans*. It controls body wall muscles and pharyngeal muscles and therefore is essential for locomotion and feeding, among other behaviors. This neurotransmitter is also implicated in neuronal activity which enables diverse functions. A single gene, *cha-1*, is responsible for the enzymatic activity that transfers the acetyl group from the acetyl-CoA to choline. Loss of function mutations in *cha-1*, result in the arrest of development and death just after hatching (Rand & Russell, 1985; Treinin & Jin, 2021), illustrating the importance of this gene for the correct functioning of cholinergic neurons. The CHA-1 protein sequence is conserved across evolution, with 90% of homology with mammals. Thanks to this, the generation of tools using CHA-1 as a marker showed that 30% of all the *C. elegans* neurons are cholinergic (Pereira et al., 2015; Treinin & Jin, 2021). For synaptic activity to occur, acetylcholine is released into the synaptic cleft. However, this neurotransmitter needs to be quickly removed to be able to continue responding to incoming stimuli. This is performed by a specialized enzyme called acetylcholinesterase (AChE), and *C. elegans* is a rather unique organism as it has as many as 4 AChE encoding genes (*ace-1,2,3,4*) (Arpagaus et al., 1998; Treinin & Jin, 2021), compared to only one AChE gene in mice (Y. Li et al., 1993).

Cholinergic motorneurons in *C. elegans* are essential for the characteristic locomotion of the worm, showing an S-shaped body during movement (Figure 1.7). This sinusoidal locomotion is based on a fine balance between the inhibitory transmissions, promoted by the GABAergic neurons that innervate the body-wall muscles, and the excitatory transmissions offered by the cholinergic neurons innervating body-wall muscles at the opposite side of the animal.

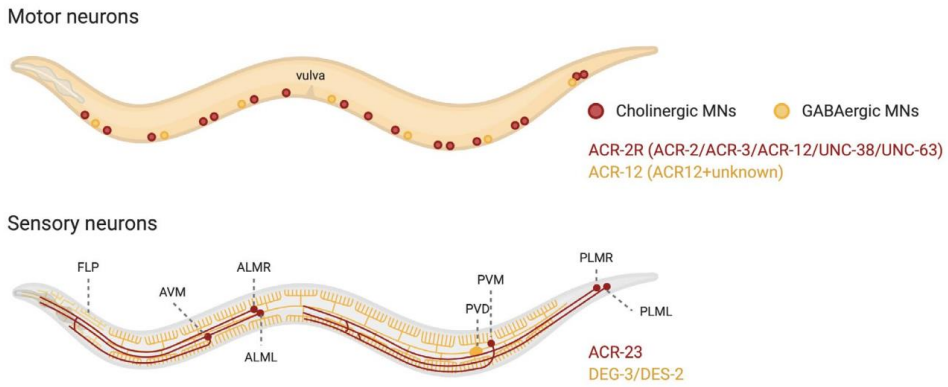

Figure 1.7: Acetylcholine-activated ion channels in *C. elegans*. Cells and receptors are colored red for Cholinergic MNs (Motor Neurons) and yellow for GABAergic MNs. Schematics of motorneurons and sensory neurons are shown. FLPR/L (Right/Left) are sensory neurons, AVM is a mechanosensory neuron, ALMR/L (Right/Left) are mechanosensory neurons, PVM is a mechanosensory neuron, PVDR/L (Right/Left) are polymodal neurons implicated in mechano- and thermosensation, and finally PLMR/L (Right/Left) are mechanosensory neurons. Image adapted from Treinin & Jin, 2021.

1.3 Uncovering new mutants in *C. elegans*

1.3.1 Genetic screens

Since *C. elegans* is a very versatile model organism, it has been widely used to study the effect of mutations, thus, creating important tools for gene function discovery. Genetic screens rely on producing and isolating mutations that allow the identification and characterization of genes involved in biological processes. Three main mutagenesis strategies are commonly used: a) Genome-wide (unknown genes that control a biological mechanism are looked for, i.e. forward genetic screens); b) Target-selected (the entire genome is mutagenized, but mutations in a single gene are screened, i.e. reverse genetics); and c) Gene-targeted (one gene is mutagenized, i.e. reverse genetics) (Kutscher & Shaham, 2014).

Sydney Brenner (1974) identified simple recessive mutations by mutagenizing wild-type worms with ethyl methane sulphonate (EMS), an alkylating agent that modifies

the nucleotides G/C to A/T, commonly producing stop codons. This component induces mutations in the sperm and oocytes, with a mutation rate of $2.5x10^{-3}$ mutations/gene/generation (Kutscher & Shaham, 2014). Using such mutagenesis, Brenner identified more than 600 mutants with visible phenotypes, such as small bodies, blistered cuticles, rolling locomotion, and long or dumpy bodies, among others. He also identified some mutations that produced neuronal defects like the *unc-30* mutants (affecting a gene now known to encode for a transcription factor that regulates neuronal fate), and *unc-6* mutants that show defects in neuronal pathfinding and axon outgrowth (Jorgensen & Mango, 2002).

Thanks to the simplicity of these genetic screens, an increasing number of scientists started using them to find novel mutants implicated in important biological processes. Some screens were used to uncover genetic modifiers by looking for enhancers or suppressors, where a mutation suppresses a particular phenotype by restoring it close or back to wild type (e.g., *lin-15* and the negative regulation in the RAS pathway (Singh, 2020)). Other screens use drug selections to find mutants with resistance or sensitivity to such drug (e.g., *unc-17* (Brenner, 1974), which is required to transport acetylcholine into the synaptic vesicle). All these kinds of genetic screens can be scaled to a larger number of worms, finding mutations that are significantly less frequent.

Some forward genetic screens have also helped to study the early development of embryos. At this stage, a homozygous embryo with a mutation in a certain gene can still normally develop using the RNAs and proteins that the heterozygous mother has donated to the egg. However, the progeny that is born from a homozygous mother with the mutation might die or present a phenotype. These genes are identified as maternal-effect mutations which are implicated in early developmental decisions. These mutations commonly generate progeny with significant diverse defects (i.e., maternal-effect uncoordinated, *mau*, mutants) and some of these, can be lethal (i.e., maternal-effect lethal, *mel*, mutants).

Importantly, all the neuronal development and function genes that were originally characterized in *C. elegans* were at first genetically defined by mutations isolated in forward genetic screens, and then characterized molecularly and mechanistically. Thus, genetic screens for mutants defective in neuronal development and/or function *in C. elegans* have been invaluable to accelerate the progress of neuroscience. Since, in general, mechanisms can be identified by studying mutants and going all the way to the cellular and molecular underpinnings of a biological process.

Particularly, in 1995, Hekimi and his lab performed a genetic screen for maternal-effect mutations, identifying numerous genes required for normal development (Hekimi et al., 1995). A schematic of this forward genetic screen is shown in Figure 1.8. To perform this genetic screen, wild-type worms (N2) were mutagenized with EMS and allowed to self-fertilize for two generations. Some behavioral and morphological phenotypes were already observed among these two first generations as expected after mutagenesis, but it was worms that showed a WT phenotype that were of interest for this screen. These wild-type-looking F2 worms were singled into new plates and allowed to self-fertilize for another generation (F3). The worms that showed a full mutant plate on the third generation were of interest. Indeed, for an entire F3 brood to appear phenotypically mutant, the mother must have been homozygote (*m/m*) for the mutation, yet this F2 animal was wild type and did not show a mutant phenotype at the F2 generation. Thus, such an F2 animal was so-called maternally rescued. In contrast, when these F2 *m/m* hermaphrodites produce their F3 progeny, the mother -being homozygous- can no longer rescue the mutation and produces F3 progeny that are genotypically homozygous for the mutation and now show the mutant phenotype. These kinds of mutants are extremely interesting to understand how maternal mRNAs function and how important they are for the correct development of the worm. Since maternal mRNAs are produced during oogenesis and stored in the oocyte until fertilization, they usually encode key regulators for early development (Rajyaguru &

Parker, 2009). These maternal mRNAs repress the zygotic transcription of the corresponding genes in early development, which allows more rapid DNA synthesis and cell cycles, promoting faster development and more intrinsic regulation.

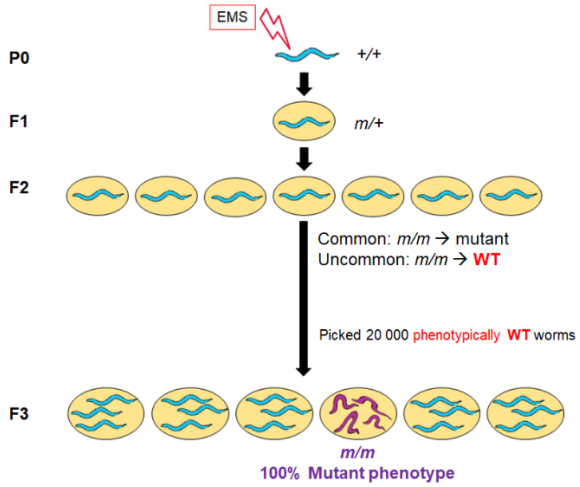

Figure 1.8: Schematic of the mutagenesis with EMS performed by the Hekimi Lab in 1995. *m* represents mutant gene, *m/+* is heterozygote, *m/m* is homozygote.

The mutants uncovered from this forward genetic screen were classified into seven phenotypic classes: 1) *mau* (maternal-effect uncoordinated); these mutants show uncoordinated movements, with high levels of embryonic (30%) and larval (30%) lethality; 2) *mum* (maternal-effect uncoordinated and morphologically abnormal); these mutants show deformed pharynx, uncoordinated movements and abnormal gonads; 3) *mal* (maternal-effect morphologically abnormal); these mutants show protrusions on the head and buccal cavity; 4) *mad* (maternal-effect dumpy); these mutants show poor embryonic elongation generating very short worms, and very slow development; 5) *mud* (maternal-effect uncoordinated and dumpy); these mutants also show very short worms and kinky uncoordination; 6) *clk* (abnormal function of biological clocks); these mutants show variable embryonic and post embryonic cycles, long lifespan and irregular behavioral rhythms like swimming and pumping; 7) genes involved in sex determination and/or dosage compensation.

The *mau* mutants, of interest in this work, were subdivided into 3 groups: (1) *mau-1, mau-2,* and *mau-4* their mutations produce neuroanatomical defects; 2) *mau-3, mau-5* and *mau-6* have defects in muscle function; and 3) *mau-7* and *mau-8* produce general locomotion defects and embryonic lethality (Hekimi et al., 1995). Among these *mau* genes, only *mau-2* has been identified so far (Takagi et al., 1997).

1.3.2 Transgenesis

Following genetic screens and the isolation of new mutants, scientists developed molecular genetics methods, like transgenesis or the generation of transgenic animals. This approach is done to carry out rescue assays and thus enabling the identification of the gene causally mutated in a new mutant strain. It also allows to manipulate individual genes, for instance by driving a gene's expression in targeted cell types and at given times during the animal's life (Nance & Frøkjær-Jensen, 2019). The most commonly used method, having helped *C. elegans* researchers for over 35 years and still being widely used, is to micro-inject a DNA mixture into the hermaphrodite germline, which results in the generation of a single extrachromosomal array harboring thousands of copies (hence it is called "multicopy") of the injected DNA vectors, which can be plasmids, fosmids, cosmids, yeast artificial chromosomes, among others (Fire, 1986). This method has some limitations such as variable expression or silencing in the germline, however, it is a very rapid and efficient tool for scientific discovery. In cases where abnormally high levels of expression interfere with normal function, new developed methods such as single-copy transgenesis, integrating extrachromosomal arrays and transgenesis mediated by transposons can be used (Frøkjær-Jensen et al., 2014; Kage-Nakadai et al., 2012; Yoshina et al., 2016). In this work, we use the classical multicopy transgenesis as well as the single-copy insertion by the MiniMos method (detailed in the Results Chapter).

Additional methods are being developed to continue improving transgenic gene expression in manners that would allow the temporal and spatial regulation of certain

proteins, among which, Auxin Induced Degradation is a recent example (Zhang et al., 2015). Molecular biology is opening doors to technical aspects that would allow to have a better understanding of intrinsic mechanisms that control the development of the organism in its entirety.

1.4 Research objectives

The work presented here focuses on three mutants of the *mau* class (*mut A, mut B and mut C*). These three mutants were recovered from a screen for maternal-effect mutations and display abnormal locomotion and neuroanatomical defects. Interestingly, these mutants display highly variable locomotion over time at the level of each individual animal. This phenotypic variability may suggest that, beyond playing a role during the development of the nervous system, these genes may play regulatory roles as well.

To better understand the implications of these genes in neuronal development and/or function, these mutants were characterized phenotypically using locomotion and pharmacological assays, as well as examining two major classes of neurons (GABAergic and cholinergic). Molecular identification was also pursued by performing a variety of rescue assays, using multiple copy transgenesis, as well as single-copy insertions. The information uncovered in this work will help understand which genes are potentially needed for the correct development of the nervous system in *C. elegans*.

CHAPTER II

MATERIAL AND METHODS

2.1 *C. elegans* strains

Nematode cultures were maintained in an incubator at 20°C (unless otherwise stated) on NGM plates seeded with *Escherichia coli* OP50 bacteria as described (Brenner, 1974). Wild-type reference strains and fluorescent markers were obtained or constructed using standard genetic procedures and are listed in Table 2.1. Genotypes were confirmed by genotyping PCR or by sequencing when needed, as established below. All the mutant alleles and reporter strains are outcrossed with the Bristol N2 wild-type strain at least 3 times prior to use for analysis or strain building.

Table 2.1: Wild-type reference strain and fluorescent markers used

Strain name	**Genotype**	**Transgene**	**Reference**
N2	Wildtype		Brenner, 1974
VQ1444	*ufIs34 II*	*unc-47p::mCherry*	Petrash et al., 2013
VQ1445	*vsIs48 X*	*unc-17p::GFP*	Chase et al., 2004
VQ84	*ufIs34 II; vsIs48 X* derived from IZ829 and LX949, respectively	*unc-47p::mCherry; unc-17p::GFP*	Petrash et al., 2013; Chase et al., 2004

2.2 Genotyping strains

To obtain DNA for PCR genotyping, DNA was extracted by lysis of the animals. This was done using lysis buffer (KCl 1M; Tris pH8.2 1M; $MgCl_2$ 1M; IGEPAL 10% stock; Tween-20 10% stock; Gelatin 5% stock). To create the final lysis buffer, 0.3 µL of Proteinase K (20mg/mL stock) is added to every 100 µL of lysis buffer. This complete lysis buffer will be used by either washing the plates of interest with 100 µL of lysis buffer, or by picking 16-25 worms in 25 µL of lysis buffer. Lysis consists of two main steps: 2 h at 60°C and 20 min at 95°C, and then the samples are kept at 10°C until use.

The genotyping PCRs are done with primers designed to recognize specific mutations: deletion alleles are assayed for with a set of three primers (two primers outside the deletion, and one inside the deletion). For genotyping point mutations, the protocol for Super-Selective PCR was used (Touroutine & Tanis, 2020). Briefly, the Super-Selective PCR consists in designing a forward or reverse primer that recognizes the point mutation on its 3' tip (either wild type or mutant version, respectively). The complementary primer (either forward or reverse) is a normal 18 bp primer. The Super-Selective PCR cycle needs to be optimized to ensure the specificity of the wild type and the mutant PCRs independently.

To confirm the homozygosity of the strains being built, worms were singled for two or more generations to confirm that all the singles have the genotyping PCR band of interest. In some cases, for final confirmation of point mutations, a PCR product that includes the point mutation and around 200 bp up and downstream of it, is sent to sequence to Nanuq Genome Quebec.

2.3 Locomotion analysis using the thrashing assay

Worms were pre-pooled at the L4 stage onto new seeded plates and then picked after ~20 h as young adults to be transferred to the scoring slide, as previously described (Nawa & Matsuoka, 2012). Briefly, worms were transferred using minimal bacterial glue, one at a time, in 8 µL of M9 solution on a microscopy slide. Their movements were immediately recorded on the dissecting microscope for 90 sec, using an iPhone camera held by a microscope objective adapter. The thrashing behavior was then categorized every 5 sec according to a set of qualitative criteria established in Table 2.2.

Table 2.2: Qualitative locomotion criteria

Color Code	Type of locomotion	Description of the movement
	Thrashing	Normal wild type thrashing from head to tail
	Coiled	The tail is turned around itself
	Pretzel	The body forms a "∞" shape
	Spasms	Sudden, intense, and major muscle contraction
	Paralysis	Absence of movement and muscle contractions
…..	Trembling	Several consecutive small muscle contractions
!	Reversals	Backward movement
	Coiled and spasms	Presence of spasms while in a coiled position
	Thrashing and spasms	Normal thrashing accompanied by spasms

2.4 Pharmacological Assays

Aldicarb and levamisole are commonly used (Mahoney et al., 2006) to study defects in cholinergic synaptic transmission by evaluating the sensitivity for one or both of these components. As described (Mahoney et al., 2006), L4 stage worms were picked the day before, in order to have young adults for the assay. All tests were done in a blinded manner. Plates with 1 mM of aldicarb and 100 µM of levamisole were prepared, and a group of 15 worms per plate were assayed. All the animals (mutants and control) were assayed in parallel. To test for paralysis, the nose and tail were tapped with an eyelash pick 3 times. In absence of response, the worm was considered paralyzed. Movement or paralysis was recorded every 15 min for 3 h.

2.5 Neuroanatomical observations

The strains were maintained at 20°C and well-fed for at least three generations prior to observation. Worms were immobilized with sodium azide (75 mM) on a pad of 5% agarose and then covered with a coverslip. Worms were observed with a fluorescence microscope Zeiss Imager M2 equipped with an AxioCam, capturing images processed by the AxioVision software. In order to examine the overall morphology of neurons in wild-type and mutant animals, fluorescent reporters were used (see Table 1 and Table 5) enabling the visualization of several subsets of neurons by fluorescence microscopy

using an upright compound microscope. New strains were generated for each of the mutants carrying a given neuronal reporter. In this work, GABAergic and cholinergic motor neurons were scored, using as a reference the wild-type neurons on the left side, as shown in Figure 2.1. Scoring criteria will be further explained in the Results section. Worms aged L4 and young adults (with 2-3 embryos) were scored.

Figure 2.1: Schematic representation of the left side of a wild-type (WT) worm. GABAergic neurons are represented in red (left) and Cholinergic neurons, in green (right). The left side of a WT worm possesses, invariably, one GABAergic commissure (corresponding to the DD1 neuron), and seven Cholinergic neurons throughout the body.

2.6 Microinjection and generation of transgenic animals

Young adult hermaphrodite worms with no more than 2-3 embryos (for wild type) and 4-5 embryos (for mutants), were mounted on halocarbon oil to constrain their movement, an eyelash pick was used to rotate the worm to have a clear sight of the gonads, as previously described (Evans, 2006; Mello et al., 1991). Prepared DNA injection mixes consist of plasmids with the cDNA of interest under a tissue-specific promoter or a YAC (with concentrations between 10ng/µL to 25ng/µL), one or more co-injection markers (10ng/µL), and $pBSK^{+}$ as filler DNA (necessary amount to complete final concentration of 250ng/µL). Needles used for injection were generated from a PC-100 (NARISHIGE) needle puller using borosilicate glass capillaries (Kwik-Fil, ID: 0.88mm, Length: 100mm, catalog n°2105334). Microinjection was executed using a Zeiss Axio Vert A.1 inverted microscope with a micromanipulator (NARISHIGE) and Femtojet (Eppendorf). The injection mix was injected into the distal gonad syncytium of the young adult hermaphrodite worm, which was then allowed to recover on a new seeded plate with a drop of M9 solution. The previously

prepared injection mixes were centrifuged at 15000 rpm for 10 min before the injection session.

Multicopy transgenes: Transgenic F1 progeny were screened under a fluorescent dissecting microscope for worms expressing the co-injection marker/s. Independent transgenic lines derived from independent F1 transgenic worms were established, which were then maintained as new strains for neuroanatomical and behavioral analysis.

Single-copy insertions (MiniMos approach): The single-copy insertion MiniMos method is performed following previous works (Frøkjær-Jensen et al., 2014), unless otherwise noted. Briefly, the MiniMos plasmids are generated by classical cloning, and were extracted with PureLink HQ Mini Plasmid kit (Invitrogen), to ensure purity and high-quality DNA for the injection mix. A series of co-injection markers, which were also extracted with the PureLink HQ Mini Plasmid kit (Invitrogen), are added to the injection mix, allowing the recognition of transgenics through positives and negatives selections, as explained below. These co-injection markers are pGH8 (P*rab-3:mCherry:unc-54 3'*UTR), pCFJ90 (P*myo-2:mCherry:unc-54 3'*UTR), pCFJ104 (P*myo-3:mCherry:unc-54 3'*UTR), pCFJ601 (P*eft-3:mos1 transposase:tbb-2 3'*UTR) and pMA122 (P*hsp16.41:peel-1:tbb-2 3'*UTR).

Three to four injected young adult P0 hermaphrodite worms are transferred to recover in new seeded plates with drops of M9 solution. These plates are incubated at 25°C for 24 h. After 24 h, 238 µL of Neomycin (25 mg/mL) are added directly to the plates containing the injected P0 hermaphrodites. This volume was poured slowly, drop by drop, and allowing the liquid to dry before adding the next batch of drops. This prevents the injected worms from being lost on the sides of the plate. Once the whole volume of the liquid is dried, the plates are sealed with parafilm and returned to the 25°C incubator to allow P0s hermaphrodites to keep laying embryos. The addition of Neomycin at this step induces the death of all the worms that do not carry the plasmid of interest, since

the worms that were successfully injected and that have the plasmid (either extra chromosomally or integrated), will be resistant to Neomycin (antibiotics resistance is encoded in the backbone of the plasmid). Plates are left at 25°C until starvation (the number of days until starvation is variable depending on the strain injected). Once starvation has been reached, the plates are heat-shocked for 2 h at 34°C, in an air incubator, and then put back at 25°C for 24 h. This heat-shock step specifically kills the worms that carry the extra-chromosomal array by activating the *peel-1* toxin (included in the pMA122 plasmid). Thus, only worms that lose the extrachromosomal arrays survive, and thus the co-injection markers on the extrachromosomal arrays are also lost. The only worms that survive are the ones that have integrated the genetic cassette of interest, which gives them Neomycin resistance (NeoR). After 24 h, the plates are screened for worms that are notably alive and, importantly, that lack all the co-injection markers (i.e., desired worms are "dark" as they lack all co-injection markers that could only be kept as part of an extrachromosomal array). These dark and alive worms are singled onto new seeded plates. Once these new plates with singled animals become populated with enough worms, worm lysis (crude DNA preparation, as detailed above) and PCR genotyping is performed to confirm the presence of the NeoR gene (Primer Fwd: 5’ ATTGCACGCAGGTTCTCC; Primer Rev: 5’GGATCAAGCGTATGCAGC), and therefore insertion of the desired transgene. Worm progeny from NeoR-positive candidate plates are singled again so as to generate a homozygous insertion strain, for which all singled progeny of one generation show the presence of the NeoR band in the genotyping. This confirms that the insertion is homozygous. The strains that are confirmed to be homozygous for the MiniMos insertion are named and frozen, and posteriorly used to perform genetic crosses into the desired mutant background. With this approach, the insertion is integrated in a random manner. Thus, to determine the location of insertion, Inverted PCR should be performed (Frøkjær-Jensen et al., 2014).

2.7 Molecular biology and generation of transgenes

2.7.1 Plasmids for multi-copy transgenesis

Plasmids for multi-copy transgenesis are generated by classical molecular cloning, assembling the cDNA or genomic sequence of interest, under the control of an upstream tissue-specific promoter and followed by a downstream 3'UTR, in a vector backbone with Ampicillin resistance. The plasmids used in this work are presented in Table 2.3. These plasmids were obtained by miniprep using PureLink HQ Mini Plasmid kit (Invitrogen) and purified with ethanol precipitation to ensure high-quality DNA for microinjection.

Table 2.3: Multi-copy plasmids used throughout this work

Plasmid Name	Transgene	Expression
pCB407	*rgef-1p::gene-X::unc-54 3'UTR*	Pan-neuronal
pCB413	*unc-47p::gene-X::unc-54 3'UTR*	GABA neurons
pCB412	*unc-17Bp::gene-X::unc-54 3'UTR*	Cholinergic neurons
pCB419	*myo-3p::gene-X::unc-54 3'UTR*	Body wall muscles
pCB418	*dpy-7p::gene-X::unc-54 3'UTR*	Hypodermis

2.7.2 Plasmids for single-copy insertion transgenes by MiniMos

The minimal Mos1 transposon (MiniMos) single-copy insertion approach is based on an independent insertion of a sequence of interest into the genome of the worm. This protocol was performed following Frøkjær-Jensen et al., 2014, with certain modifications. Briefly, the transgene or sequence of interest is inserted into pCFJ910 MiniMos vector (which contains the Minimal Mos1, Neomycin Resistance, and a Multiple cloning site) by classical cloning using the restriction enzyme sites in the MCS of the vector, as seen in Table 2.4. With these plasmids of interest, then the MiniMos protocol is followed (see 2.6, *Single-copy insertions*).

Table 2.4: Single-copy plasmids used throughout this work

Plasmid Name	Transgene	Expression
pCB461	*rgef-1p::gene-X::unc-54 3'UTR*	Pan-neuronal
pCB476	*gene-Xp::gene-X::gene-X 3'UTR*	*gene-X* endogenous expression

2.8 Statistical analyses

All the statistical analyses were done using GraphPad Prism. The results presented in the figures are expressed as the mean ± standard error of the mean, or proportion ± standard error of the proportion. Values for genotypes were compared by t-test (for numerical values such as means) or z-test (for categorical values such as proportions). The p-values considered significant were < 0,05 (*), 0,01 (**) and 0,001 (***).

CHAPTER III

RESULTS

3.1 Phenotypical characterization of three novel neuronal mutants

3.1.1 Analysis of locomotion: *mut A, mut B and mut C* mutants display abnormal locomotion patterns

Behavioral analysis allows the study of locomotion patterns and certain specific aspects of the mutants' phenotypes, which can be informative regarding the function of the genes under study. Abnormal locomotion is a very common characteristic of neuronal mutants with misguided motorneurons, and it is readily observed on the culture plates of *mut A, mut B and mut C* mutants under study. However, these mutants have the particularity that they appear to display variability over time within a given individual (Claire Bénard, unpublished observations). To characterize their locomotory variability, we video recorded and then quantified behavioral features, by performing thrashing assays. From the 90 seconds recording of the worms' thrashing in liquid, pictures were selected to illustrate stereotypical body posture differences between wild-type animals and *mau* mutants, as shown in Figure 3.1.

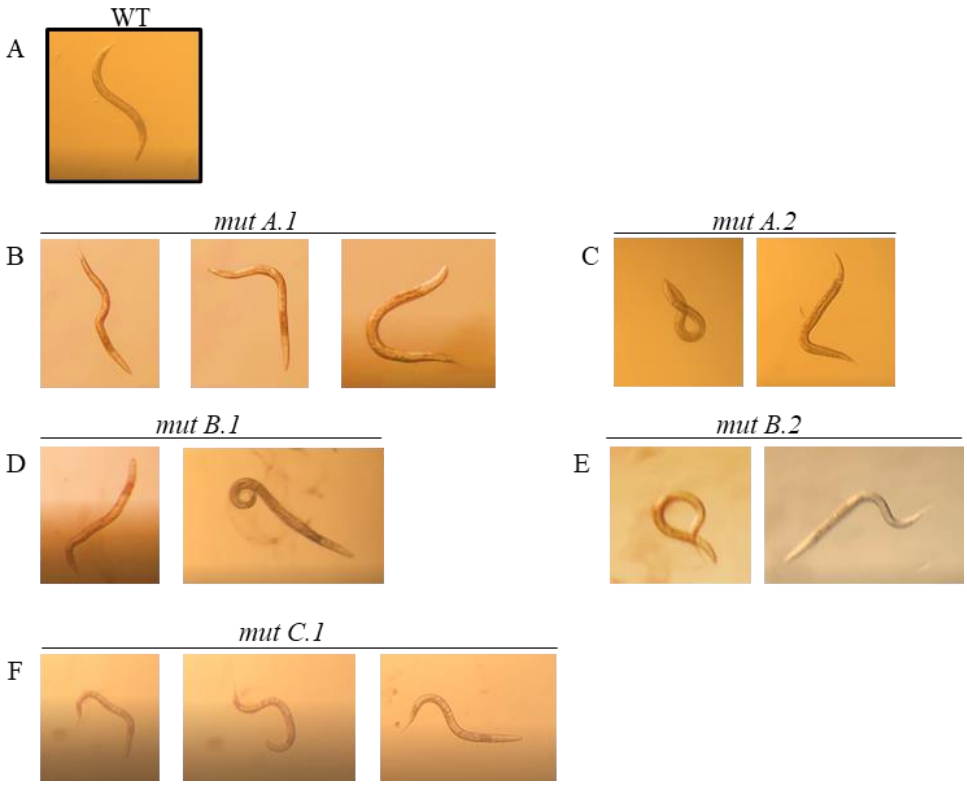

Figure 3.1: Pictures extracted from video recordings of the locomotion thrashing behavior for each strain. A) wild type (WT), B) *mut A.1*, C) *mut.A.2*, D) *mut B.1*, E) *mut B.2* and F) *mut C.1*. The wild-type strain shows the normal sinusoidal body shape, whereas all the *mau* mutants show kinked-shaped bodies, some coiled around their body and the presence of parts of the body completely straight, while another part of the body with a hooked or coiled tail. There are no significant changes in size between mutants, the apparent size change is due to change of focus of the camera. Every frame for each mutant represents the same worm at different times within the 90 second essay interval. All these images are of adult worms that measure ~ 1 mm long. The body size of mutants *mut A.1*, *mut A.2*, *mut B.1* and *mut B.2* is very similar to that of wild-type animals, whereas *mut C.1* worms are slightly smaller.

As expected, wild-type worms were able to thrash continuously during the 90 sec interval, with smooth movements, and without any trembling or paralysis. This is considered a normal thrashing and is the qualitative reference for analyzing locomotion in the mutants. In contrast, we found that *mut A, mut B and mut C* mutants generally fail to show a normal sinusoidal body, rather presenting bodies that are completely straight, or with parts of the body hooked or kinked. Some of the mutants *mut A, mut B and mut C* also show extreme coiling of either certain parts of their body or of the entire body. The pictures shown in Figure 3.1, are of the same corresponding mutant worm taken at different seconds of the 90 seconds interval thrashing assay. They clearly show the intrinsic variability of the locomotion behavior within one independent worm.

A batch of 10 worms for each *mut A, mut B and mut C* mutant strains was scored in these thrashing assays, following the set of criteria established in Material and Methods. These qualitative results (Figure 3.2) show how *mut A.1* and *mut A.2* attempt to thrash at the beginning of the assay, maintaining thrashing locomotion for 5 seconds or as long as 25 seconds. This might be related to an immediate escaping mechanism since we see something similar when mutant worms are touched with a pick in the solid plates. Although they immediately react to the touch, and move backwards, a couple of seconds later, they go back to their uncoordinated physical appearance. This escape response might be related to observing the thrashing through the first couple of seconds in the liquid media. However, once this fades, the mutant worms start to tremble, showing signs of spasms and even paralysis. It appears that *mut A.2* is less severely affected as it thrashes more frequently, but still shows spasms, trembling, and paralysis. In the case of the *mut B.1* and *mut B.3* mutants, both show frequent spasms, with almost continuous trembling and periods of paralysis. Interestingly, *mut B.3* seems to have more frequent periods of attempts of thrashing compared to *mut B.2*. This mutant shows a coiled body more frequently compared to *mut B.2*. Finally, *mut C.1* shows the most severe thrashing defects compared to the other mutants studied, spending most of the time paralyzed throughout the 90 seconds, with lapses of time with spasms that end up

in paralysis. These results show that all mutants, despite differences, display severe thrashing defects. In addition, there is an individual variation over time, especially in the most intense phenotypes, oscillating between complete paralysis and spasms, or between trying to thrash and have a coiled-shaped body. Although these results are qualitative, they allowed us to appreciate unusual phenotypic differences in the mutants (as compared to the dozens of other uncoordinated mutants known to worm neurobiologists) and suggest that the genes mutated in these strains might have regulatory roles.

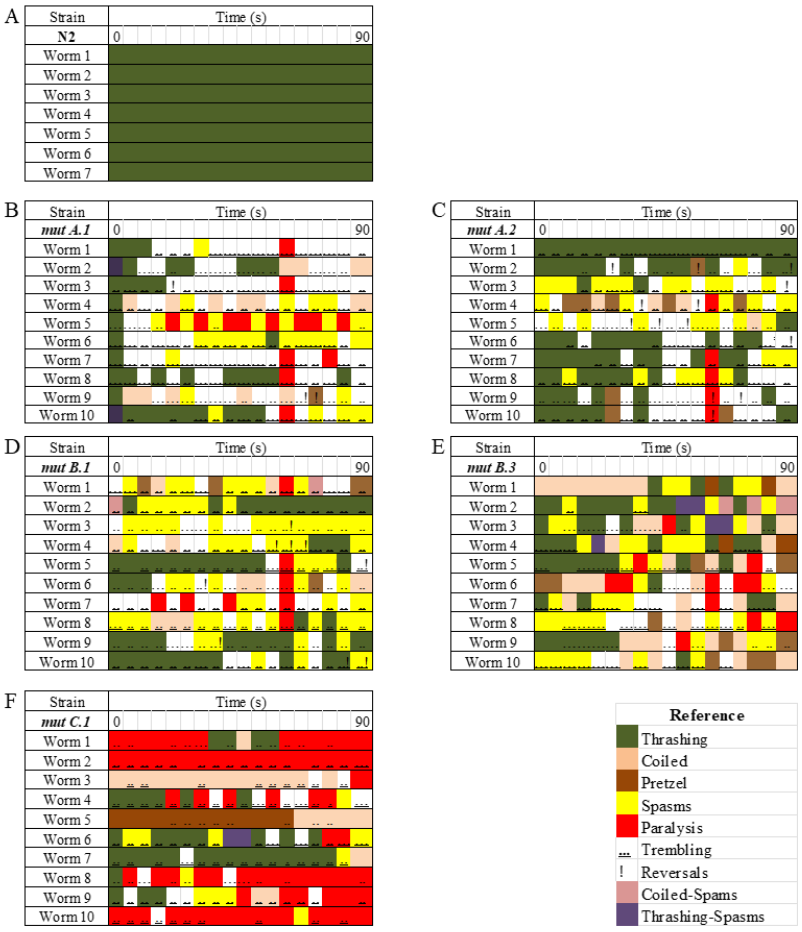

Figure 3.2: Qualitative thrashing quantification of WT and *mau* mutants. A) wild type (N2), B) *mut A.1*, C) *mut A.2*, D) *mut B.1*, E) *mut B.3*, F) *mut C.1*. The locomotion behavior corresponding to each color is represented in the Reference table. WT worms show normal thrashing (dark green) throughout 90 sec. Whereas *mau* mutants

show independent and intrinsic variability, showed by the presence of different locomotion patterns (i.e different colors), throughout time.

3.1.2 Pharmacological assays: *mut A, mut B and mut C* mutants have abnormal responses to drugs that allow to test synaptic transmission

To determine whether mutants *mut A, mut B and mut C* have defective synaptic transmission, pharmacological assays were performed. Briefly, aldicarb is an acetylcholinesterase inhibitor. In the presence of aldicarb, acetylcholine accumulates in the synaptic cleft leading to overactivation of cholinergic receptors, generating muscle hypercontraction, paralysis, and death. Levamisole is a cholinergic agonist, which exerts its therapeutic effect by potentially activating one of the two cholinergic receptor types in body-wall muscles. This leads to muscle hypercontraction, paralysis, and death. By combining the data obtained with these two pharmacological components, the location of the defect can be readily detected. If a mutant worm is resistant to aldicarb but not to levamisole, then the affected gene probably functions in the pre-synapse. Conversely, if the mutant worm is resistant to both drugs, the defect is probably due to alterations in the post-synapse.

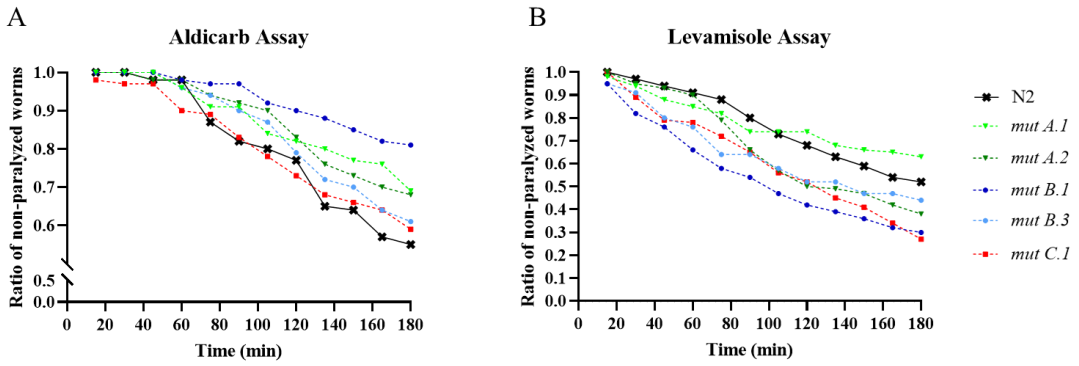

Figure 3.3: Results of the Aldicarb and Levamisole pharmacological assays. The axis represents the ratio of non-paralyzed worms throughout the 180 min of experimentation. Wild type worm (N2) is represented as a full black line, the rest of the *mau* mutants are represented with dotted lines. Green dotted lines correspond to *mut A.1* and *mut A.2*, blue dotted lines correspond to *mut B.1* and *mut B.3*, and finally, red dotted line corresponds to *mut C.1*. A) Aldicarb assay, B) Levamisole assay.

In general, we found that all mutants *mut A, mut B and mut C* are resistant to aldicarb (Figure 3.3, A), as all of their curves are above the wild-type animals' full black line. *mut B.1* shows the most resistance to aldicarb, maintaining a relatively high ratio of non-paralyzed worms. Whereas *mut C.1*, shows the same tendency of resistance as a wild-type worm. On the other hand, all the mutants seem to be sensitive to levamisole (Figure 3.3, B), although *mut A.1* shows a slight increase above the wild type at around 150 min. Considering these results, since mutants are resistant to aldicarb but sensitive to levamisole, this suggests that the affected genes probably function in the pre-synapse of cholinergic neurons. Therefore, this initial result suggests that these mutants have pre-synaptic defects.

3.1.3 Neuroanatomy analysis: *mut A, mut B and mut C* mutants display morphological defects in GABAergic and cholinergic neurons

To examine the overall morphology of neurons in wild-type and mutant animals, we used fluorescent reporters enabling the visualization of several subsets of neurons by fluorescence microscopy using an upright compound microscope. New strains were generated for each of the *mut A, mut B and mut C* mutants carrying a given neuronal reporter, as described in Material and Methods, which are shown in Table 3.1.

Table 3.1: Mutant strains generated for this study

Strain name	Genotype	Reference
VQ1236	*mut A.1*	Hekimi et al., 1995
VQ1196	*mut A.2*	Hekimi et al., 1995
VQ1137	*mut B.1*	This work
VQ1759	*mut B.2*	This work
VQ1264	*mut B.3*	This work
VQ1064	*mut C.1*	This work
VQ1437	*mut A.1; ufIs34 II*	This work
VQ1438	*mut A.1; vsIs48 X*	This work
VQ1016	*mut A.1; ufIs34 II; vsIs48 X*	This work
VQ1835	*mut A.2; ufIs34 II*	This work
VQ1473	*mut B.1; ufIs34 II*	This work
VQ1474	*mut B.1; vsIs48 X*	This work

VQ1767	*mut B.2; ufIs34 II*	This work
VQ1846	*mut B.3; ufIs34 II*	This work
VQ1468	*mut C.1 ufIs34 II*	This work

In wild-type animals, GABAergic and cholinergic motorneurons have a characteristic and invariant pattern (Figure 3.4, A), resulting from each of their axons extending from the cell body, which is located on the ventral midline of the animal, along the body wall, and all the way to the dorsal nerve cord. Most GABAergic axons migrate on the right side of the animal's body. In the case of GABAergic and cholinergic motorneurons, while neuronal identity and axon outgrowth are normal, mutants *mut A, mut B and mut C* display significant guidance defects, which can be grouped into two main defects: mid-line guidance defects (Figure 3.4, B) and lateral guidance defects (Figure 3.4, C). The mid-line guidance defects consist of the presence of extra commissures, either GABAergic or cholinergic, on the left side of the worm. These commissures appear to leave the ventral nerve cord and reach its final target (the dorsal nerve cord) normally, albeit through the wrong side of the body of the worm. Due to the characteristic structure of neurons in *C. elegans*, since they are monopolar, the mid-line guidance defects might be related to a defect in the sense of growing direction. It appears that the neuron exits the ventral cord towards its target, however, it grows towards the dorsal nerve cord through the left side of the worm rather than the right side. However, since the right side of the worm is very crowded with GABAergic neurons, it is very difficult to know if these extra commissures are formed from an erroneous decision of left vs right. Another case, although rare, would be if the commissure on the left side, still has its counterpart on the right side of the worm. The lateral guidance defects are based on the presence of commissures that not only have they made the wrong side decision (i.e left side, rather than the correct right side) but they also present the characteristic of not arriving to the dorsal nerve cord. These defects show commissures with T-shapes (Figure 3.4, C), sometimes following

laterally the ventral nerve cord through the middle of the left side of the worm, and sometimes also forming stomps barely leaving the ventral nerve cord.

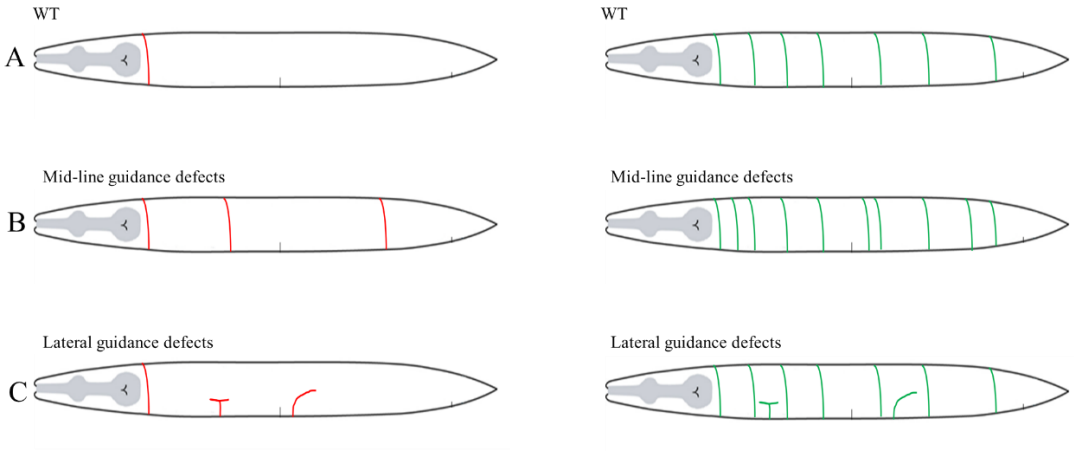

Figure 3.4: Schematic of the left side of the worm, showing GABAergic neurons in red (left schematics) and cholinergic neurons in green (right schematics). Wild-type worm (WT) (A), invariably show one GABAergic commissure and 7 cholinergic commissures on the left side of their body. Mutant strains have shown most frequently two types of defects: mid-line guidance defects (B) and lateral guidance defects (C). The GABAergic fluorescent marker is *ufIs34 [unc-47p::mCherry]* and the Cholinergic fluorescent marker is *vsIs48 [unc-17p::GFP]*.

Neuroanatomical examination was performed on L4 or young-adult worms (ideally no more than 3-4 embryos; N<100 worms per strain) to evaluate GABAergic and Cholinergic neurons, using strain *ufIs34* in the wild-type background as control of the normal disposition of GABAergic and Cholinergic neurons. As can be seen in Figure 3.5, all the mutant strains have significant differences compared to the wild type for the midline guidance defects. Regarding lateral guidance defects, only *mut C.1* shows significant differences with the wild type. Finally, *mut A.1*, *mut B.1*, *mut B.2*, and *mut C.1*, showed significant differences with wild type, in the presence of both midline and lateral guidance defects.

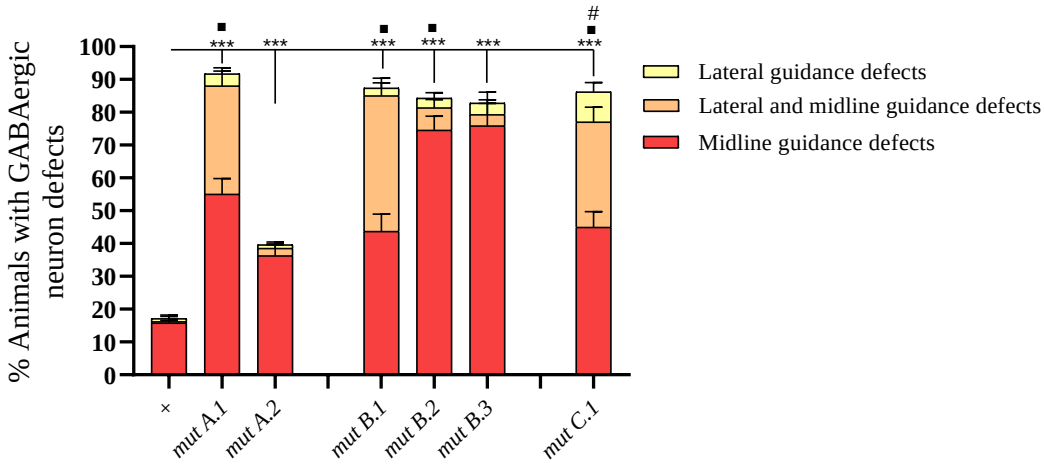

Figure 3.5: Neuroanatomical defects observed in all mutants using marker *ufIs34*, which allows the visualization of GABAergic motorneurons. The percentage of animals with GABAergic neuron defects is classified into two main categories: Midline guidance defects (red) and Lateral guidance defects (yellow), as well as animals displaying both types of defects (orange). Significant differences were obtained by Z-tests and differences between the wild-type and mutants were represented using (*) midline guidance defects, (▪) lateral and midline guidance defects, and (#) lateral guidance defects. The absence of a specific icon represents no significant differences for that defect.

The same type of scoring was performed by evaluating the cholinergic neurons on the left side of the worm. The classification of defects was maintained (midline or lateral guidance defects), considering that the left side of the worm generally has 7 cholinergic commissures, 4 anterior to the vulva, and 4 posterior to the vulva. Only *mut A.1* and *mut B.1* were examined in this case since we already had these strains previously built with the cholinergic marker and having a reference of two different mutants was enough to gain insight into cholinergic defects (Figure 3.6). Both of these mutants show significant differences with the wild type for the midline guidance defects and the presence of both defects (i.e midline and lateral guidance defects).

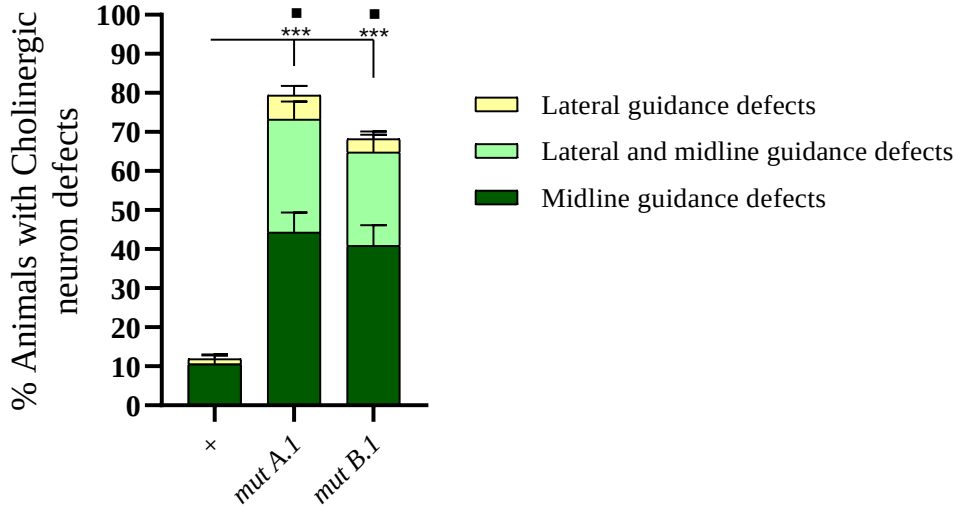

Figure 3.6: Neuroanatomical defects observed in all mutants using *vsIs48* marker (+), which allows the visualization of Cholinergic motorneurons. The percentage of animals with Cholinergic defects is classified into two main categories: Midline guidance defects (dark green) and Lateral guidance defects (yellow), as well as animals displaying both types of defects (light green). Significant differences were obtained by Z-tests and differences between the wild-type and mutants were represented using (*) midline guidance defects, (▪) lateral and midline guidance defects, and (#) lateral guidance defects. The absence of a specific icon represents no significant differences for that defect.

3.2 Towards the molecular identification of the genes corresponding to *mut A, mut B and mut C*

The mutations described above have interesting neuronal defects that are worth pursuing to decipher cellular and molecular mechanisms responsible for neuronal development and function. The first crucial step to understanding their function is the identification of the genes responsible for the mutant phenotypes in the *mut A, mut B and mut C* strains. For this, data from classical genetic mapping (Hekimi 1995, C. Bénard unpub. results), combined with whole-genome resequencing and bioinformatic analyses (C. Bénard with the help of Dr. M. Doitsidou) allowed to generate a short list of most likely candidates (Figure 3.7), which were tested with rescue assays. These

candidates have different nature of mutations. The first, *gene-X*, has two mutant alleles, *mut A.1* which is a point mutation (represented by the head of the arrow) and a deletion mutation, *mut A.2* (represented by the square bracket). The second, *gene-Y*, has three mutant alleles, one point mutation (*mut B.1*) and two deletion mutations (*mut B.2* and *mut B.3*). Finally, *gene-Z*, has only one mutant allele, with a point mutation (*mut C.1*).

The key assay to determine whether a candidate gene with the verified mutation is indeed the one responsible for the mutant phenotypes in the mutants *mut A, mut B and mut C* is to conduct rescue assays. In these assays, mutant animals are provided with transgenic wild-type copies of the candidate gene and are examined for reversion of the defects. If transgenic mutant animals now display a wild-type behavior and/or neuroanatomy, then the gene responsible for the defects has been unequivocally identified.

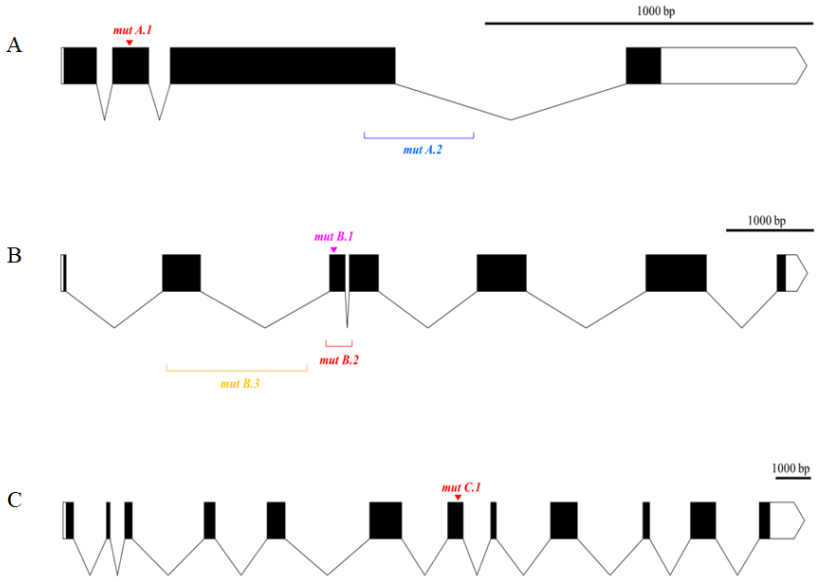

Figure 3.7: Scheme of the three main genes of interest in this work. A) *gene-X* with alleles *mut A.1* and *A.2*, B) *gene-Y* with alleles *mut B.1*, *B.2* and *B.3*, C) *gene-Z* with a single allele, *mut C.1*. Arrowheads represent point mutations and square brackets represent deletions. Black-filled boxes represent exons, and triangular lines in between black boxes represent introns. White boxes at the beginning and end of the sequence represent the 5' and 3' UTRs respectively.

3.2.1 Molecular identification of *gene-X*

From the whole-genome sequencing candidate list, the genomic locus of *gene-X* has been previously tested by Andrea Thackeray and Claire Bénard at the University of Massachusetts Chan Medical School. The genomic locus was obtained by PCR and injected into the worm generating a multi-copy transgenic line. This line showed positive behavioral rescue, with decreased larval and embryonic lethality, increased growth rate, and normal locomotion. However, neuroanatomy was not studied in these worms.

Next, tissue-specific promoters can be used to determine the site of action of the gene under study. Thus, multi-copy plasmids carrying transgenes to express *gene-X* under tissue-specific promoters were generated by the interest in rescuing the phenotype in a particular tissue. Here, we wanted to know if *gene-X* would rescue if the wild-type copy of the gene were expressed in all neurons, GABAergic neurons, Cholinergic neurons, body wall muscles, and hypodermis, as shown in Table 3.2. The full-length cDNA of *gene-X* was cloned under the respective tissue-specific promoters (*rgef-1p* [pan-neuronal], *unc-47p* [GABAergic neurons], *unc-17B* [Cholinergic neurons], *myo-3p* [body wall muscle], and *dpy-7p* [hypodermis]; work done by Lise Rivollet in the Bénard lab), followed by the 3'UTR of the heterologous gene *unc-54*, which is commonly used in *C. elegans* rescue assays. We also tested the PCR genomic region previously obtained by Andrea Thackeray, to generate a multi-copy line. These plasmids were micro-injected into the gonad of hermaphrodites *mut A.1*, and transgenic lines carrying injected multiple copy plasmids (~10 000 copies) were generated by selecting for the co-injection marker, as shown in Table 3.3.

Table 3.2: List of multi-copy plasmids and their tissue-specific expression

Plasmid Name	Transgene	Expression
pCB407	*rgef-1p::gene-X::unc-54 3'UTR*	Pan-neuronal
pCB413	*unc-47p::gene-X::unc-54 3'UTR*	GABA neurons
pCB412	*unc-17Bp::gene-X::unc-54 3'UTR*	Cholinergic neurons
pCB419	*myo-3p::gene-X::unc-54 3'UTR*	Body wall muscles
pCB418	*dpy-7p::gene-X::unc-54 3'UTR*	Hypodermis

Table 3.3: Established multi-copy transgenic lines used for thrashing and neuroanatomical scoring

Strain name	Genotype	Plasmid injected	Co-injection markers
VQ1521	*mut A.1; ufIs34 II;qvEx455 Line 1*	*[rgef-1p::gene-X] 25 ng/µL*	*cc::GFP 50 ng/µL; pBSK 125 ng/µL*
VQ1522	*mut A.1; ufIs34 II;qvEx456 Line 2*	*[rgef-1p::gene-X] 25 ng/µL*	
VQ1523	*mut A.1; ufIs34 II;qvEx457 Line 3*	*[rgef-1p::gene-X] 25 ng/µL*	
VQ1524	*mut A.1; ufIs34 II;qvEx458 Line 1*	*[unc-47p::gene-X] 25 ng/µL*	
VQ1525	*mut A.1; ufIs34 II;qvEx459 Line 2*	*[unc-47p::gene-X] 25 ng/µL*	
VQ1526	*mut A.1; ufIs34 II;qvEx460 Line 1*	*[dpy-7p::gene-X] 0.5 ng/µL*	
VQ1527	*mut A.1; ufIs34 II;qvEx461 Line 2*	*[dpy-7p::gene-X] 0.5 ng/µL*	
VQ1528	*mut A.1; ufIs34 II;qvEx462 Line 3*	*[dpy-7p::gene-X] 0.5 ng/µL*	
VQ1551	*mut A.1; ufIs34 II;qvEx468 Line 1*	*[myo-3p::gene-X] 5 ng/µL*	
VQ1552	*mut A.1; ufIs34 II;qvEx469 Line 1*	*[unc-17Bp::gene-X] 25 ng/µL*	
VQ1553	*mut A.1; ufIs34 II;qvEx470 Line 2*	*[unc-17Bp::gene-X] 25 ng/µL*	
VQ1554	*mut A.1; ufIs34 II;qvEx471 Line 3*	*[unc-17Bp::gene-X] 25 ng/µL*	
VQ1555	*mut A.1; ufIs34 II;qvEx472 Line 1*	*[unc-47p::gene-X] 5 ng/µL*	*cc::GFP 50 ng/µL; lgc-11::GFP 30 ng/µL;*
VQ1556	*mut A.1; ufIs34 II;qvEx473 Line 2*	*[unc-47p::gene-X] 5 ng/µL*	

VQ1579	*mut A.1; ufIs34 II;qvEx477 Line 1*	*[rgef-1p::gene-X] 5 ng/µL*	*pBSK 115 ng/µL*
VQ1580	*mut A.1; ufIs34 II;qvEx478 Line 2*	*[rgef-1p::gene-X] 5 ng/µL*	
VQ1581	*mut A.1; ufIs34 II;qvEx479 Line 3*	*[rgef-1p::gene-X] 5 ng/µL*	
VQ1728	*mut A.1; ufIs34 II;qvEx556 Line 1*	*[gene-X locus] 7.9 ng/µL*	*cc::gfp 40 ng/µL; lgc-11::GFP 40 ng/µL ;* bacterial digested genome *100 ng/µL*
VQ1750	*mut A.1; ufIs34 II;qvEx562 Line 2*	*[gene-X locus] 7.9 ng/µL*	
VQ1754	*mut A.1; ufIs34 II;qvEx564 Line 3*	*[gene-X locus] 7.9 ng/µL*	

The transgenic lines obtained from the different multi-copy plasmids were evaluated for rescue considering their thrashing behavior and the neuroanatomy scoring. The results obtained from the thrashing assays are shown in Table 3.4, where only the pan-neuronal (*rgef-1p*) and GABAergic (*unc-47p*) promotors could fully rescue the thrashing back to wild-type. The behavioral rescue was confirmed when worms are back to showing sinusoidal movements, without spasms, paralysis, or any other mutant phenotype as per established in the behavioral scoring criteria. However, the expression of the gene of interest either in the hypodermis (*dpy-7p*) or only in body wall muscles (*myo-3p*) did not rescue behavior. A partial behavioral rescue was obtained when the gene of interest was expressed under the cholinergic neuron promotor (*unc-17Bp*). The expression of *gene-X* only in body wall muscles or in the hypodermal syncytium, under the expression of the *myo-3* promotor or the *dpy-7* promoter, respectively, is not enough to rescue the phenotype, suggesting that *gene-X* might be needed in different tissues simultaneously. However, the fact that a pan-neuronal promoter (*rgef-1*) rescues thrashing behavior, suggests that *gene-X* has a different and important function in neurons, where the sole presence of wild-type copies of the gene (not even with its own promotor nor 3’UTR) is enough to rescue locomotion.

Table 3.4: Thrashing assay results for *mut A.1* transgenics with different multi-copy plasmids

Mutant strain	Multicopy plasmids (Expression)	Thrashing rescue?
mut A.1	*rgef-1p::gene-X::unc-54 3'UTR* (Pan-neuronal)	Yes
	unc-47p::gene-X::unc-54 3'UTR (GABAergic neurons)	Yes
	unc-17Bp::gene-X::unc-54 3'UTR (Cholinergic neurons)	Partially
	myo-3p::gene-X::unc-54 3'UTR (Body wall muscles)	No
	dpy-7p::gene-X::unc-54 3'UTR (Hypodermis)	No

Beyond rescue at the locomotion and overall growth rate levels, all these transgenic lines were also analyzed to evaluate neuroanatomy defects, considering midline and lateral guidance defects. As shown in Figure 3.8, the transgenic lines with the pan-neuronal promoter (*rgef-1p*), hypodermis promoter (*dpy-7p*), cholinergic neurons (*unc-17Bp*), and the whole genomic locus of *gene-X*, did not show significant differences with *mut A.1*, thus indicating an absence of rescue of neuroanatomical defects. However, expression of *gene-X* in GABAergic neurons (*unc-47p*) shows significant differences with *mut A.1*, for the midline guidance defects. The expression in muscles (*myo-3p*) also shows significant differences with *mut A.1*, regarding midline and lateral and midline guidance defects. This suggests that *gene-X* might be important for the neuronal interaction with body wall muscle. However, the absence of thrashing rescue with the same promoter indicates that there are other tissues where *gene-X* is needed to fully rescue the phenotype.

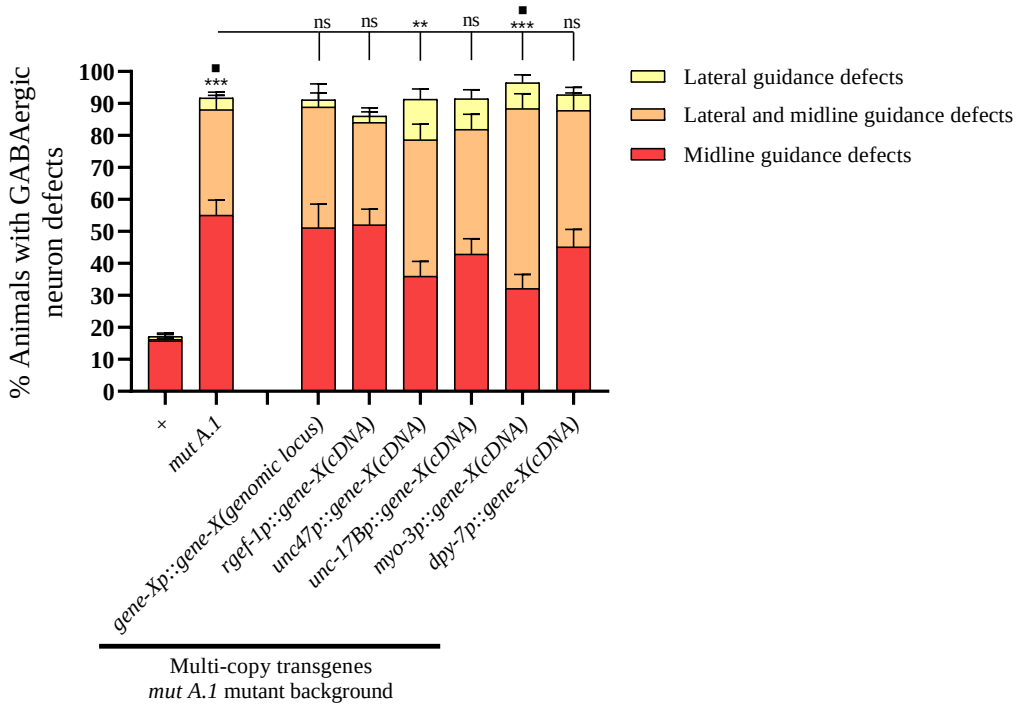

Figure 3.8: Neuroanatomical defects observed in all multiple copy transgenic lines in *mut A.1* background, using *ufIs34* marker (+), which allows the visualization of GABAergic motorneurons. The percentage of animals with GABAergic neuron defects is classified into two main categories: Midline guidance defects (red) and Lateral guidance defects (yellow), as well as animals displaying both types of defects (orange). Significant differences were obtained by Z-tests and differences between *mut A.1* and the transgenic lines in *mut A.1* background were represented using (*) midline guidance defects, (▪) lateral and midline guidance defects, and (#) lateral guidance defects. The absence of a specific icon represents no significant differences for that defect. n.s refers to non-significant differences.

Since multiple copies of *gene-X* seem to impede the correct rescue of *mut A.1*, it is likely that this gene is extremely well regulated, and thus needs a nearly endogenous dosage and the presence of its own regulatory elements. This guided us to build single-copy transgene insertion strains, using the MiniMos approach, as described in Materials and Methods. This approach allows having close to the endogenous level of expression of the gene of interest. For this, I built plasmids of interest (Table 3.5) using the

pCFJ910 MiniMos backbone, which has Ampicillin and Neomycin resistance. The single-copy insertion strains thus established are shown in Table 3.6.

Table 3.5: Plasmids created using the pCFJ910 MiniMos backbone vector for single-copy insertion

Plasmid Name	Transgene	Expression
pCB461	*rgef-1p::gene-X::unc-54 3'UTR*	Pan-neuronal
pCB476	*gene-Xp::gene-X::gene-X 3'UTR*	*gene-X* endogenous expression

Table 3.6: Single-copy (MiniMos) established lines and used for scoring.

Question marks represent the lack of knowledge of the location of the inserted transgene

Strain name	Genotype	Plasmid injected	Co-injection markers
VQ1802	*qvTi3*	*[rgef-1p::gene-X] 10 ng/µL*	*pGH8 10 ng/µL; pCFJ90 2.5 ng/µL; pCFJ104 10 ng/µL; pCFJ601 50 ng/µL; pMA122 10 ng/µL*
VQ1813	*qvTi4*	*[rgef-1p::gene-X] 10 ng/µL*	
VQ1827	*qvTi4 ?; ufIs34 II*	*[rgef-1p::gene-X] 10 ng/µL*	
VQ1865	*mut A.1; qvTi3 ?; ufIs34 II*	*[rgef-1p::gene-X] 10 ng/µL*	
VQ1821	*mut A.2; qvTi3 ?; ufIs34 II*	*[rgef-1p::gene-X] 10 ng/µL*	
VQ1915	*qvTi5*	*[gene-X locus] 10 ng/µL*	
VQ1916	*qvTi6*	*[gene-X locus] 10 ng/µL*	
VQ1917	*qvTi7*	*[gene-X locus] 10 ng/µL*	
VQ1942	*qvTi7 ?; ufIs34 II*	*[gene-X locus] 10 ng/µL*	
VQ1963	*mut A.1; qvTi7 ?; ufIs34 II*	*[gene-X locus] 10 ng/µL*	

The single-copy insertions of *gene-X* under the control of the pan-neuronal promoter showed a significant improvement in the locomotion and general aspect in both

mutant backgrounds. However, this plasmid does not manage to rescue neuroanatomical defects in either *mut A.1* nor *mut A.2* background, showing non-significant differences with their corresponding mutant reference (Figure 3.9). Interestingly, when the entire genomic locus of *gene-X* (*gene-Xp::gene-X [genomic]::gene-X 3'UTR*), is inserted in the *mut A.1* background, this shows a clear and total rescue of the neuroanatomy defects, showing significant differences for the midline and lateral and midline guidance defects (Figure 3.9).

These complete rescue results of all evaluated phenotypes confirm that the mutations in *gene-X* are responsible for the defects observed in *mut A.1* and *mut A.2*. It thus appears that *gene-X* is a very well-regulated gene in the worm and that the presence of its own regulatory elements (i.e promoter and 3'UTR), as well as transgenic expression at levels similar to endogenous, are both important for the function of this gene.

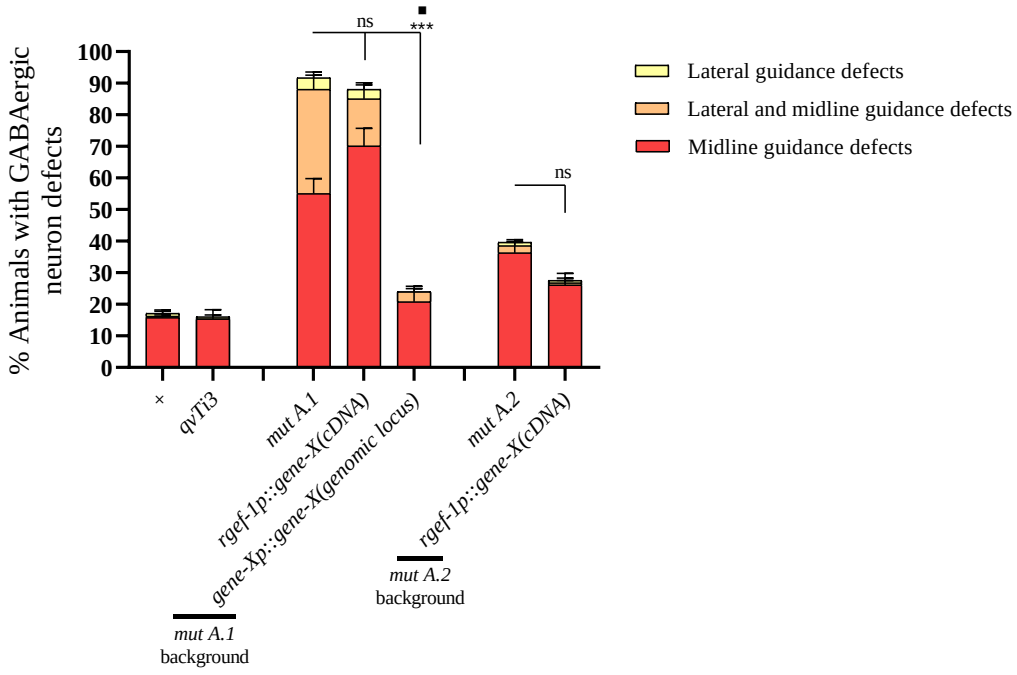

Figure 3.9: Neuroanatomical defects observed in all single-copy transgene inserted lines in *mut A.1* and *mut A.2* background, using *ufIs34* marker (+), which allows the

visualization of GABAergic motorneurons. An additional control is shown (*qvTi3*), which is the single-copy inserted line in a wild-type background. The percentage of animals with GABAergic neuron defects is classified into two main categories: Midline guidance defects (red) and Lateral guidance defects (yellow), as well as animals displaying both types of defects (orange). Significant differences were obtained by Z-tests and differences between *mut A.1* or *mut A.2* and their corresponding single-copy insertions in the mutant background were represented using (*) midline guidance defects, (▪) lateral and midline guidance defects, and (#) lateral guidance defects. The absence of a specific icon represents no significant differences for that defect. n.s refers to non-significant differences.

3.2.2 Molecular identification of *gene-Y*

To work towards the molecular identification of *gene-Y*, two approaches were considered based on the previous results with *gene-X*. Due to the size of the genomic locus of *gene-Y* (~8 300 bp), the fact that it is the second gene of an operon, and the repetitive nature of the DNA sequence, this was prohibitive for successful PCR amplification. Thus, obtaining the whole genomic sequence of interest would be problematic. Following the approach pursued with *gene-X*, we considered using the cDNA of *gene-Y* and expressing it under a ubiquitous promoter such as *sur-5p* or under a pan-neuronal promoter as *rgef-1p*. These sequences would then be followed by the heterologous 3'UTR of the gene *unc-54*.

Alternatively, considering the information obtained from rescuing of the *gene-X* above, where all the regulatory sequences (i.e endogenous promoter and 3'UTR), as well as expressing at nearly endogenous levels (using a single copy, as opposed to multiple copies of the transgene) were the only ones conferring a full rescue of the neuroanatomical defects, we designed a molecular cloning strategy accordingly (Figure 3.9.1). After several unsuccessful attempts of PCR amplifying parts of the genomic sequence of *gene-Y*, we decided to build a *gene-Y* "minigene" made partly of cDNA and partly of genomic sequence. This minigene contains the cDNA of *gene-Y* from the start codon until exon 6, followed by genomic sequence corresponding to exon 6 until the end of 3'UTR of *gene-Y*. This second genomic part was synthesized by IDT.

The detailed strategy would be as follows. Initially, the cDNA of *gene-Y* until exon 6, would be cloned in the pBSK backbone to generate a relatively small plasmid. The IDT synthesized sequence is provided in an AmpR plasmid by the company. By classical cloning, using several of restriction enzymes, these two fragments would be assembled in the pBSK backbone. On the other side, the promoter of *gene-Y* obtained by PCR amplification using nested PCR, would be cloned into the pCFJ910 MiniMos backbone. With these two plasmids in hand, the last cloning pursued would be to assemble the minigene into the pCFJ910 plasmid that has the promoter of *gene-Y*. This would finally allow us to have a plasmid containing the endogenous promoter of *gene-Y*, the complete sequence of *gene-Y*, and its own 3'UTR.

Cloning efforts are currently ongoing as this thesis is being written. The *gene-Y* minigene plasmid has been completed and sequenced to confirm there were no mutations that could have arisen from the PCR amplification and/or cloning. The optimization of the PCR to amplify the promoter of *gene-Y* is ongoing. We hope to be able to obtain single-copy transgene insertions for *gene-Y* very soon.

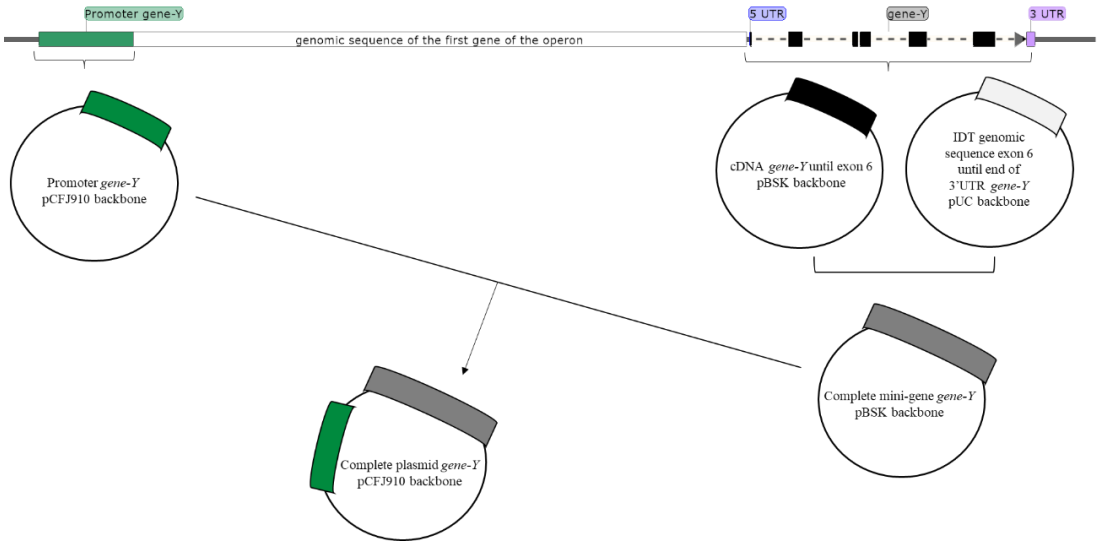

Figure 3.9.1: Cloning design to build the plasmid containing the promoter, mini-gene (cDNA plus genomic sequence) and 3'UTR of *gene-Y* in single-copy pCFJ910

MiniMos backbone. The promoter of *gene-Y* is represented in dark green. The cDNA of *gene-Y* until exon 6, obtained from a previously designed plasmid is represented in black. The genomic sequence starting at exon 6 until the end of the 3'UTR of *gene-Y* synthesized by IDT is represented in light grey. The assembly of the whole mini-gene (i.e the cDNA of *gene-Y* plus the rest of the genomic sequence) is represented in dark grey. The completed plasmid in the pCFJ910 MiniMos backbone has the promoter and the mini-gene of *gene-Y*. Full genomic sequence created in SnapGene.

3.2.3 Molecular identification of *gene-Z*

Similar to *gene-Y*, *gene-Z* has an even bigger genomic sequence (~ 21 kb) and is also part of an operon. Due to the absence of a full-length cDNA for *gene-Z*, through WormBase, we found a Yeast Artificial Chromosome (YAC) that carries *gene-Z* in its entirety, and a second gene of the operon. In order to favor recombination of these large pieces of microinjected DNA for multi-copy extrachromosomal arrays, we digested the YAC with the restriction enzyme PstI (which linearizes the YAC increasing its capacity to form extrachromosomal arrays, without cutting *gene-Z*) and injected it with co-injection markers, into the *mut C.1* background.

All the multi-copy transgenic lines obtained from injecting the YAC showed complete rescue of the locomotion behavior and growth rate of *mut C.1* (data not shown). As a reminder, *mut C.1* is the mutant that displays the most severe locomotion thrashing patterns, with paralysis during most of the 90 sec thrashing assays (Figure 3.2). These rescued lines showed worms with normal sinusoidal body shapes, constant movement, and no signs of paralysis nor spasms. However, again, neuroanatomical defects were not rescued by this YAC containing *gene-Z* (Figure 3.9.2) since it does not show significant differences with *mut C.1*. Given that a large portion of the promoter of *gene-Z*, its entire sequence, with all its introns, as well as its 5' and 3' UTRs are all contained in the YAC, this suggests again that the levels of expression are key for this gene's function, and that multiple copies affect the dosage and therefore prevent normal function.

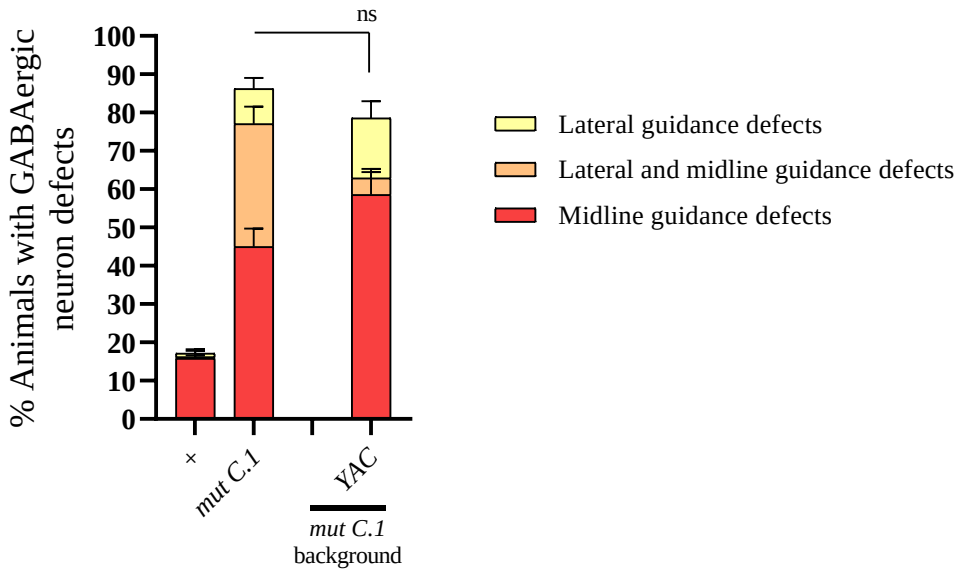

Figure 3.9.2: Neuroanatomical defects observed in the multiple-copy line with the YAC in *mut C.1* background, using *ufIs34* marker (+), which allows the visualization of GABAergic motorneurons. The percentage of animals with GABAergic neuron defects is classified into two main categories: Midline guidance defects (red) and Lateral guidance defects (yellow), as well as animals displaying both types of defects (orange). Significant differences were obtained by Z-tests and differences between *mut C.1* and the multiple-copy transgenic line were represented using (*) midline guidance defects, (▪) lateral and midline guidance defects, and (#) lateral guidance defects. The absence of a specific icon represents no significant differences for that defect. n.s refers to non-significant differences.

CHAPTER IV

DISCUSSION

In this work, we characterized some mutants that were obtained from a forward genetic screen performed by the Hekimi Lab in 1995. These mutants, namely *mut A, mut B,* and *mut C,* have the particularity of being maternally rescued, meaning that they only show a mutant phenotype in the second homozygous generation. This phenotypic maternal rescue is likely due to the presence of wild-type, non-mutated, copies of the gene's transcripts in the oocyte, which are thus transferred from the mother to the zygote, enabling to rescue its development. The main phenotypes observed in these mutants (Hekimi et al., 1995) are uncoordinated locomotion, partial embryonic and larval lethality, among others. This work focused on characterizing these mutants considering their locomotion (through thrashing behavior), defects in synaptic transmission (through pharmacological assays), and defects in GABAergic and cholinergic motorneurons morphology (through neuroanatomical observations). Also, rescue assays were performed using multiple or single-copy transgenes for the molecular identification of candidate genes.

4.1 *mut A, mut B,* and *mut C* mutants show locomotion defects and individual variability over time

Related to the locomotion of these mutants, Claire Bénard had noticed a certain variability of locomotion through time within individual animals. Thus, to study the locomotion variability of these mutants, we performed thrashing assays. Briefly, this assay consists in studying the movement of an individual worm in a drop of a liquid, for 90 seconds. These thrashing assays showed that a wild-type worm, as expected, thrashes normally for the 90 second interval, constantly showing a sinusoidal-shaped body (Figure 3.1 and 3.2). However, the mutants under study showed abnormal movements (Figure 3.1 and 3.2). Mutant *mut A.1* and *mut A.2* managed to thrash

normally for the first couple of seconds, followed by trembling, and sometimes even paralysis. For *mut B.1* and *mut B.3*, locomotion is slightly more severely affected, with increased spasms, trembling, and coiled-shaped bodies. These mutants also lack the ability to thrash normally; and if they do, a normal thrashing might last only a couple of seconds, followed by a series of spasms or paralysis. Finally, *mut C.1* is the most affected mutant, with major locomotion defects: animals can be paralyzed for most of the 90 seconds interval, with intermittent seconds of spasms, occasional thrashing (for no more than a couple of seconds), and constant trembling. Regardless of the particularities of each mutant, all of them share the characteristic of individual variability over time. That is to say, not only does every worm move differently (independently of the mutation), but every independent worm changes its locomotion behavior throughout the 90 seconds assay. Interestingly, this qualitative thrashing assay allowed to confirm the individual variability of these mutants throughout time. This suggests that the mutants under study might have mutations in genes that have important regulatory roles within the neuromuscular system.

These interesting qualitative thrashing results incite us to plan for potential and future quantitative assays. While working with these mutants, we have realized that although the thrashing behavior shows significant physical locomotory distress, certain movements seen in liquid media are not seen in solid plates. In solid media most of the mutants are seen as clearly uncoordinated, barely moving throughout the plate, and in some cases, showing a completely straight body shape, with no response to stimuli (for example, *mut C.1*). Interestingly, the spasms observed in the thrashing assays, are not seen in solid plates. This raises the question if there is any mechanism that is either activated or turned off based on the physical environment the worm is exposed. Also, while feeding the worms every week, we have seen subtle changes in behavior once the worm develops into its different life stages. That is to say, most of the mutants show a relatively “normal” locomotion behavior throughout the stages L1 and L2, and once the worm starts to grow significantly in size (i.e. stage L3 onwards), the uncoordinated

phenotype is more clearly shown. Although this observation is very qualitative, there might be an interesting link between the molecular mechanisms that are affected in these mutants, with the correct development of the worm. Hence, the bigger the worm gets in size, the more difficult it is for compensatory pathways to regulate molecular mechanisms to counteract the lack of the genes that are mutated. To study this, we will analyze locomotion behavior in solid plates, considering different life stages. To obtain quantitative results, we are looking into collaborating with Dr. Alkema who has a lab specialized in behavioral analysis, with the use of the WormLab equipment (MBF Bioscience). Briefly, WormLab is a software that images, tracks, and analyzes *C. elegans* locomotion behavior. It possesses a developed algorithm that can collect information from independent or multiple worms and recognize different movements such as turns, reversals, and coils, as well as thrashing and swimming. All these movements are also complemented with information about the speed, body area and length, direction, bending angles, and more. Potentially, these quantitative results will give us more information about specific movements, and variations within time and within an individual worm, allowing us to further characterize the specific effects of the mutations of these genes in each mutant.

4.2 *mut A, mut B,* and *mut C* mutants might have defects in the pre-synapse of cholinergic neurons

Due to the phenotypical characteristics of the *mut A, mut B,* and *mut C* mutants, we next examined whether these mutants might have synaptic transmission defects. For this, we performed pharmacological assays, exposing the worms to aldicarb (acetylcholinesterase inhibitor) and levamisole (cholinergic agonist) and evaluating the effect on the worms over a period of 3 hours (Figure 3.3). The evaluation of paralysis of worms allows determining the resistance or sensitivity to either drug and helps to elucidate if the alterations are predominantly pre- or post-synaptic. All the mutants studied here showed resistance to aldicarb (Figure 3.3, A) since the rate of non-paralyzed worms is higher than wild-type worms. Related to the specific resistance to

aldicarb, *mut B.1* seems to have the strongest resistance, showing the highest percentage of non-paralyzed worms compared to the rest of the mutants. On the other hand, all the mutants are sensitive to levamisole (Figure 3.3, B), shown by the presence of lower rates of non-paralyzed worms compared to wild type. In conclusion, the mutants analyzed were sensitive to levamisole. Taken together, it appears that the function of the genes affected in these mutants is particularly important in the pre-synaptic compartment, of cholinergic neurons in this case, rather than in the post-synaptic or muscle compartment. One might have expected for this type of gene that all cell types would be equally affected (and indeed in addition to displaying uncoordinated locomotion, all these mutant strains have a degree of embryonic and larval lethality). However, the results of the pharmacological assays point to a particularly high sensitivity of neurons in these mutants, in comparison to other tissues. Since these mutants show neuronal guidance defects but no gross morphological defects in the muscles, as observed by Normarski microscopy and polarized light as described in Hekimi et al. (1995), it seems plausible to consider that neurons seem to be more affected by the mutations in these housekeeping genes. Indeed, neurons seem to be particularly sensitive to stresses that affect their overall proteostasis (Giandomenico et al., 2021; L. Li et al., 2021; Ravanidis et al., 2018). Also, numerous genes encoding RNA metabolism are mutated in neurodegenerative conditions, suggesting a link between RNA levels, distribution, action and function with the cellular physiology of neurons in particular. For instance, in relation to their highly polarized morphology, neurons are unique in possessing an additional type of RNA-protein complex or ribonucleoparticle, namely the neuronal transport granules (Batish et al., 2012; El Fatimy et al., 2016; Formicola et al., 2019), which are not present in other cell types.

Future studies could include studying morphological defects at the dendrite and sub-dendrite levels, allowing us to understand if the candidate genes are implicated in the correct localization of even smaller structures within the neurons. This could be

performed by obtaining or producing fluorescent markers that specifically label certain parts of the dendrites like receptors. Subsequently, the composition of dendrites could be of interest. Since the candidate genes might be related to mRNA decay pathways, the disruption of these molecular mechanisms might have significant effects on the normal composition of molecules in dendritic compartments. We could analyze this by tagging a series of proteins or molecules that are present normally in dendrites, and then analyze the variability within mutants. This will help us understand how our candidate genes might be affecting parallel molecular mechanisms, and potentially which are being directly regulated by our genes.

4.3 *mut A, mut B,* and *mut C* mutants have GABAergic and cholinergic morphological defects

Since *mut A, mut B,* and *mut C* mutants show locomotion defects, we then proceeded to analyze the main motor neurons that oversee locomotion: GABAergic and cholinergic neurons. For this, we built several strains (Table 3.1), with fluorescent markers that label GABAergic (*ufIs34 [unc-47p::mCherry]*) and cholinergic (*vsIs48 [unc-17p::GFP]*) neurons. Due to the presence of numerous neurons on the right side of the worm, we decided to look at the left side of the worm where neurons and commissures are more easily recognizable. On the left side of a wild-type worm (Figure 3.4, A), there is only one GABAergic commissure which corresponds to the DD1 neuron, which extends through the left side of the worm, going towards the dorsal nerve cord close to the bulb of the pharynx. With respect to cholinergic neurons, there are seven commissures on the left side of a wild-type worm, usually four before the vulva and 3 after the vulva.

For *mut A, mut B,* and *mut C* mutants under study, we found two predominant defects in these GABAergic and cholinergic neurons. The first kind of defect is termed the “midline guidance defect” (Figure 3.4, B). This defect consists of the presence of extra commissures for each type of motor neuron on the left side of the worm. These commissures appear to leave the ventral nerve cord on the left side and reach its final

target, which is the dorsal nerve cord. Although we cannot be certain if this commissure on the left side means that the neuron made an incorrect decision on the ventral nerve cord and instead of going through the right side of the body, it decided to go through the left; or the neuron created an extra commissure and now the neuron became bipolar (which is not common in *C. elegans*). For further experiments, neuron-specific promoters should be found for GABAergic neurons, which would allow us to recognize if the extra commissure is because its counterpart is lacking on the right side or is it because the neuron became bipolar. In this work, the midline guidance defects have been based solely on the fact that there are extra commissures on the left side of the worm that should not be there.

The second type of defect is called the "lateral guidance defect" (Figure 3.4, C), where neurons have made the wrong decision of going to the left side, but these commissures do not appear to reach the final target in the dorsal nerve cord. These commissures usually show random structures like T-shapes, stomps, or even very long extensions throughout the body, but never reach the dorsal nerve cord. Finally, the third criterion for neuroanatomy scoring is the presence of both types of major defects in an individual worm, which will be called "midline and lateral guidance defects". Figure 3.5 shows the neuroanatomy scoring of GABAergic motorneurons, for each one of the mutants studied in this work. All the mutant strains show significant differences compared to wild type for each of the defects. When comparing *mut A.1* and *mut A.2*, *mut A.1* has significant differences both for midline and lateral and midline guidance defects compared to WT. However, *mut A.2*, only has significant differences for the midline guidance defects. This might suggest that there is a difference in severity in the effect of the mutation in *mut A.1* (point mutation) versus *mut A.2* (deletion). Since the point mutation in *mut A.1* is located in the second exon of the genomic sequence and generates a stop codon, this might lead to the absence of the protein encoded by *gene-X*. However, the deletion mutation in *mut A.2* affects the end of exon 3 and a great part of the last intron of *gene-X*. This suggests that this mutation might still be able to

produce the protein but with the last exon missing. For the group of *mut B*, *mut B.1* and *B.2* show significant differences with wild type regarding the midline and lateral and midline guidance defects, compared to *mut B.3* which only shows significant differences in the midline guidance defects. Finally, and complementing the results of thrashing, *mut C.1* is the only mutant that has significant differences with wild type in the three categories of neuroanatomy scoring, showing that these mutants are more severely affected than the rest of the mutants under study. The same type of scoring was done with *mut A.1* and *mut B.1* using the cholinergic fluorescent marker, *vsIs48* (Figure 3.6). These two mutants show significant differences for midline and lateral and midline guidance defects when compared to wild type.

In this work, we have shown that *mut A*, *mut B*, and *mut C* mutants under study show significant defects in GABAergic and cholinergic neurons. For further characterization of these mutants, future studies could examine the effect of these mutations in chemosensory, mechanosensory neurons, and ventral and dorsal nerve cords, among others. Some very preliminary results performed by Lise Rivollet at the lab (data not shown) show that *mut A.2* indeed has defects in the ventral nerve cord and in the PVM neuron (mechanosensory). However, due to problems with the fluorescent marker, the N value is low. Thus, future experiments will focus on finding good fluorescent markers for specific sensory neurons, and ventral and dorsal nerve cords, to evaluate the presence of defects in each mutant. This in-depth characterization of different kinds of neurons will help to understand how broad the effect of the mutations in these genes is. Potentially, this could uncover neurons that are either more sensitive or more resistant to the lack or presence of these mutated genes.

4.4 *Genes-X, -Y, and -Z* need to be well-regulated, as they appear to depend on dosage and the presence of regulatory elements

The *mut A*, *mut B*, and *mut C* mutants studied in this work have interesting phenotypical and neuroanatomical characteristics, which incited us to pursue the molecular identification of the mutated genes. For this, previous work of whole genome

sequencing and bioinformatic analyses (Doitsidou et al., 2016) offered us a set of most likely candidates that are responsible for these mutant phenotypes (Figure 3.7). To confirm this, rescue assays were performed. These assays consist in providing a wild-type copy of the candidate gene in mutant animals, generating transgenic worms. If these transgenic animals manage to reverse the mutant phenotype into a wild-type phenotype, then the gene responsible for the defects has been molecularly identified. The transgenesis in this work can be divided into two main approaches: multi-copy transgenesis where the sequence of interest is injected into the worm and is maintained as a multiple copy extrachromosomal array; and single-copy insertions following the MiniMos protocol where the sequence of interest will be inserted as a single copy in a random site of the genome.

To molecularly identify *gene-X* we built a series of multi-copy plasmids that carry the cDNA of *gene-X*, under the control of different tissue-specific promoters; we also tried the whole genomic locus of *gene-X* (Table 3.2). Each plasmid was injected into the worm with an injection mix that also contains co-injection markers to recognize transgenic worms. We used promoters that would allow us to express pan-neuronally (*rgef-1p*), GABAergic neurons (*unc-47p*), cholinergic neurons (*unc-17Bp*), body wall muscles (*myo-3p*) and hypodermis (*dpy-7p*). Several transgenic lines were generated using each one of these promoters, as can be seen in Table 3.3. These transgenic lines were then evaluated regarding their locomotion behavior and neuroanatomy defects. We found that the pan-neuronal expression of the multi-copy plasmid manages to rescue locomotion by showing normal thrashing (Table 3.4) but does not rescue neuroanatomy (Figure 3.8), with an absence of significant differences with the *mut A.1* mutant. When expressed in GABAergic neurons, there is a rescue of locomotion, and there is a slight difference regarding the midline guidance defect compared to *mut A.1*. This might suggest that although the rescue is not complete, *gene-X* might have a different impact on independent tissues, highlighting the importance of this gene in GABAergic neurons. In the case of expression in cholinergic neurons, as well as using

the whole *gene-X* genomic cassette, none of these show significant differences to *mut A.1*, thus showing no neuroanatomical rescue. Interestingly, the expression in muscles shows significant differences regarding the midline and lateral and midline guidance defects compared to *mut A.1*. This suggests that *gene-X* might be important for the interaction between neurons and muscles. However, the fact that the expression in muscles does not rescue locomotion, makes this hypothesis unclear and suggests that *gene-X* might be needed in other tissues simultaneously.

Since multi-copy transgenesis did not offer conclusive answers, we considered that the presence of multiple copies of the wild-type gene might be interfering with the rescue. This might mean that *gene-X* is a very well-regulated gene and where only the correct dosage (i.e endogenous) might show molecular rescue. Also, although the entire genomic cassette did not show rescue, we think that the presence of regulatory elements, like its own promoter and 3'UTR, might be important to express the transgene at a nearly endogenous level. To test this, we followed the MiniMos protocol (see Materials and Methods) which consists of the single-copy insertion of the sequence of interest in a random site of the genome. For this, we built a series of plasmids containing the sequence of interest either under the expression of a pan-neuronal promoter or directly the entire genomic locus containing the promoter, the genomic sequence, and the 3'UTR of *gene-X* (Table 3.5). With this protocol, we generated several strains that possess the sequence of interest as a single copy somewhere in the genome (Table 3.6). From these strains, we performed the same neuroanatomy scoring and following statistical tests (Figure 3.9). When the MiniMos single copy plasmid under the pan-neuronal promoter is injected either in the *mut A.1* or *mut A.2* background, it does not show rescue of the neuroanatomy defects, since it shows no significant differences with its mutant counterpart. Interestingly, when the genomic locus of *gene-X* (i.e *gene-Xp::gene-X (genomic)::gene-X 3'UTR*), is injected into *mut A.1* background, it finally manages to show significant differences regarding midline and lateral and midline guidance defects compared to the *mut A.1* counterpart.

For all of the single-copy inserted lines, worms seem to move normally, with less embryonic and larval lethality. Although we did not perform thrashing assays with these lines, the locomotion recovery is obvious seeing the improvement in movement in solid plates. Importantly, this result not only confirms the neuroanatomical rescue and thus the molecular rescue, but it also suggests how essential near to endogenous expression of this gene is. As is known in the worm community, multicopy transgenesis is known to produce thousands of copies of the extrachromosomal array, however, when following a single-copy transgenesis, we reduce the number of copies to one, or in rare cases, two. This allows us to consider that single-copy insertions are nearly endogenous levels. Also, the fact that the pan-neuronal expression did not manage to rescue neuroanatomy, confirms that this gene needs to be regulated under its own regulatory elements (promoter and 3'UTR), and needs to be expressed in all of its corresponding targets, in order to have the correct dosage expression of *gene-X* as well as the tissue specificity.

Given what we learned from the molecular identification of *gene-X*, we performed similar assays with *gene-Z*. However, *gene-Z* has a significant size, making it difficult to find a full-length cDNA to design plasmids under the expression of tissue-specific promoters. Using the WormBase Database, we found a YAC that has the genomic sequence of *gene-Z*, plus other genes. We injected the digested YAC into the worm to perform multi-copy transgenesis and evaluate molecular rescue. Interestingly, the locomotion behavior appears completely rescued back to wild type, but we found no significant differences compared to *mut C.1* regarding neuroanatomy defects (Figure 3.9.2). Although we did not evaluate quantitatively embryonic and larval lethality, transgenic worms showed a growth rate similar to wild type, reaching an almost starved plate after 3-4 days (whereas *mut C.1* shows starvation after almost 2 weeks). This result is encouraging since locomotion and growth rate were clearly rescued. We suggest that the absence of neuroanatomy rescue could due to dosage, such as was seen for *gene-X*.

Based on the results of this work, we could suggest some follow-up experiments that could offer more conclusive answers about the molecular identification of *gene-Y* and *gene-Z*. By showing that regulatory elements are important for the expression of the genes of interest, we suggest obtaining the promoter and 3'UTRs for *gene-Y* and *gene-Z*. Due to the potential role of these genes, we might find them located in operons, thus having to design nested PCRs or mini-gene plasmids to be able to obtain all the genomic cassettes of interest. This is currently being pursued for *gene-Y*. With the endogenous genomic cassette for each corresponding gene, MiniMos approach would be used to maintain the lowest and close to endogenous expression of these genes. We expect this approach to offer more conclusive answers regarding rescue, not only by rescuing locomotion but also by rescuing neuroanatomy. If the efforts for obtaining the regulatory elements from *gene-Y* and *gene-Z* are not successful, another approach could be used for each gene: using CRISPR (Clustered Regularly Interspaced Short Palindromic Repeats)/Cas9 technology, a strain could be obtained where the wild-type sequence of the candidate gene is modified such that it would now carry the mutation present in the candidate gene. If the phenotype of the CRISPR-modified or mutant strain shows the same locomotion and neuroanatomical defects as our mutants, then this would constitute a strong confirmation that the mutations in the genes of interest are causal to the phenotype and this would lend solid support to our gene identification. Taking a genome editing approach by CRISPR/Cas9 would readily but solely confirm the molecular identity of the candidate genes. Indeed, as compared to rescue assays by transgenesis, genome editing does not allow any further molecular manipulation of gene expression in certain cells and/or at given times of the animals's life, and thus does not provide the opportunity to gain mechanistic insights into the mode of action of the gene. We thus decided to first use the rescue assays method, since it is widely used by the *C. elegans* community and offers more mechanistic information than genome editing by CRISPR.

4.5 Candidate genes might be linked to mRNA decay

The molecular identification of the candidate genes suggests a link of the mutants studied to mRNA decay. Since these pathways are evolutionarily conserved, the information obtained might help understand neurodevelopmental mechanisms in humans. One neuroanatomical feature which will be interesting to study in these mutants is the development and maintenance of dendritic spines in the DD GABAergic neurons. Recent studies (Cuentas-Condori et al., 2019; Cuentas-condori & Miller, 2020; Philbrook et al., 2018) have revealed that *C. elegans* possesses dendritic spines, including in the DD neurons. Thus, the worm, like flies, mice, and humans, harbors synaptic boutons at the tip of the dendritic spine, offering one more layer of synaptic regulation. We have shown that mutants *mut A, mut B* and *mut C* show guidance defects in GABAergic neurons, which likely result in locomotory defects. Besides these neurite developmental defects, it would be interesting to study if dendritic spines are also affected. Given preliminary results by a former student (D. Oliver, at UMass Chan Medical School) a small number of worms for *mut A.1* indicate that this mutant may have defective dendritic spines (reduced number, abnormal distribution, and morphology). A systematic analysis of dendritic spine morphology should be performed on *mut A, mut B and mut C* in the future, using spinning-disk confocal microscopy, following the method described by Cuentas-Condori et al., 2020. Defects in the number, distribution, and shape of the dendritic spines can be classified. In the long-term, an in-depth analysis of the molecular mechanisms regulating dendritic spine development and/or maintenance may allow to shed light on the importance of mRNA decay on neurodevelopmental disorders like autism spectrum, and early-onset schizophrenia.

Characterizing how disruption of mRNA decay genes affects the development of the nervous system, and in turn, elucidating how mRNA decay genes are regulated in normal cell function, is one of the main objectives for these future studies. Controlled spatial and temporal depletion of the genes of interest will enable to uncover the

consequences of an acute loss of their function. For this, auxin-induced degradation (AID) of the proteins encoded by *gene-X, gene-Y* and *gene-Z* (Zhang et al., 2015) could be done in GABAergic neurons. This method uses the expression of a degron ligase (TIR-1) induced by auxin, specifically in GABAergic neurons (using *Punc-47::tir-1*). Once TIR-1 is activated, it recognizes the degron sequence in the targeted protein and degrades it. Thus, we would insert the degron tag in the gene of interest by CRISPR, and then expose transgenic worms to auxin from stage L3 up to the young adult stage (no auxin on control animals). After exposure to auxin, phenotypes are examined, and GABAergic neurons isolated by Fluorescence-Activated Cell Sorting (FACS). Subsequently, RNA would be extracted from isolated neurons and sent for RNA-sequencing. Thanks to bioinformatic analyses, transcripts with markedly increased or decreased levels will be uncovered indicating what genes are regulated by the gene under study. A similar analysis could also be performed on neurons isolated from mutant strains, which would correspond to a chronic gene loss of function (as opposed to acute with AID above). Information obtained from RNA-seq would then need to be validated by a series of experiments to test the functional relevance of the results. For instance, RNA interference (RNAi) and mutant analyses of genes whose regulation was most markedly affected could be performed to test the behavioral response and the neuroanatomical consequences. While this is all in the plans for GABAergic neurons, even more targeted analyses could be done on DD neurons specifically. In this case, the six DD neurons (DD1-DD6) of *C. elegans* could be isolated, which would eliminate background noise during the analysis (compared to 26 GABAergic neurons).

CONCLUSIONS AND PERSPECTIVES

In this work, some of the *mau* mutants uncovered in a forward genetic screen performed by the Hekimi Lab (1995) - namely *mut A, mut B,* and *mut C* - were characterized phenotypically and molecularly. Thrashing assays showed that all these mutants show individual variability over time in their abnormal locomotion. This suggests that the mutated genes may have important regulatory roles, as opposed to simply resulting in a stereotypical miswiring that gives fixed locomotion defects. Further, the pharmacological response of these mutants suggests that the genes in question might affect the pre-synaptic compartment. Finally, GABAergic and cholinergic motor neurons in these mutants display midline and lateral guidance defects.

We progressed toward the molecular identification of the corresponding genes with rescue assays, using multiple-copy and single-copy transgenes. For *mut A.1,* whereas multiple-copy transgenes expressed pan-neuronally or in GABAergic neurons for the candidate gene fully rescued locomotion and growth rate, neuroanatomy was not. This might suggest that the presence of multiple copies of *gene-X* affects its correct regulation or function due to an abnormally high gene copy number. Thus, single-copy transgenes of the gene of interest (*gene-X*) were used to express close to endogenous levels. A single-copy transgene expressing the gene pan-neuronally rescued locomotion and growth rate, but again not neuroanatomy in the *mut A.1* and *mut A.2* backgrounds. In contrast, when a single-copy of the whole wild-type genomic locus of the gene (i.e with its own endogenous promoter, entire coding sequence including all exons and introns, and its 3'UTR) successfully rescued all the defects in *mut A.1* background (still to be done for *mut A.2*). This indicates that the dosage and the presence of regulatory elements, such as promoter sequences, introns, and 3'UTR, are essential for the adequate expression and regulation of *gene-X*.

For the molecular identification of *gene-Z*, we performed rescue assays using a YAC containing the candidate gene for *mut C*. We obtained growth rate and locomotion rescue; however, neuroanatomical defects were not rescued. Based on the results obtained from *gene-X*, we suggest that the failure to obtain neuroanatomical rescue is likely due to the high gene dosage and the absence of its own regulatory elements. Current efforts are focused on obtaining the regulatory elements (i.e promoter and 3'UTRs) of *gene-Y*, for further molecular cloning and MiniMos insertion. Similar efforts will be performed for *gene-Z*, with the hope that this will finally confirm the molecular identification of *gene-Y* and *gene-Z*.

Potentially, the information revealed by these proposed analyses and other future work will allow a better understanding of how the brain and neurons develop by shedding light on the implicated molecular mechanisms. This will help understand how the fined-tuned regulation of mRNA decay affects the development of neurons and dendritic spines. It is further expected that studying such conserved cellular and molecular mechanisms underlying neuronal development in the worm, may eventually help provide information to detect, alleviate or treat some neurodevelopmental diseases which may open new diagnostic and therapeutic avenues.

BIBLIOGRAPHY

Arpagaus, M., Combes, D., Culetto, E., Grauso, M., Fedon, Y., Romani, R., & Toutant, J.-P. (1998). Acetylcholinesterase genes in the nematode Caenorhabditis elegans. *Journal of Physiology (Paris)*, *92*:363–367.

Bargmann, C. I. (2006). Chemosensation in C. elegans. *WormBook : The Online Review of C. Elegans Biology*, 1–29.

Barr, M. M., & Garcia, L. R. (2006). Male mating behavior. *WormBook : The Online Review of C. Elegans Biology*, 1–11.

Batish, M., van den Bogaard, P., Kramer, F. R., & Tyagi, S. (2012). Neuronal mRNAs travel singly into dendrites. *Proceedings of the National Academy of Sciences*, *109*(12):4645–4650.

Brenner, S. (1974). The Genetics of Caenorhabditis elegans. *ChemBioChem*, *4*(8): 683–687.

Chalfie, M., Tu, Y., Euskirchen, G., Ward, W., & Prasher, D. (1994). Complex gene conversion events in germline mutation at human minisatellites for gene expression Genetic analysis of Rough sheatbi developmental mutants of maize. *Science*, *263*(5148):802–805.

Chen, L., Wang, Y., & Gao, S. (2020). Minimum number of synaptic vesicles for the initiation of a single action potential at C. elegans neuromuscular junction. *MicroPublication Biology*, *C*:8–10.

Cheung, B., Arellano-Carbajal, F., Rybicki, I., & de Bono, M. (2004). Soluble Guanylate Cyclases Act in Neurons Exposed to the Body Fluid to Promote C. elegans Aggregation Behavior. *Current Biology*, *14*:1105–1111.

Chisholm, A. D., Hutter, H., Jin, Y., & Wadsworth, W. G. (2016). The genetics of axon guidance and axon regeneration in caenorhabditis elegans. *Genetics*, *204*.

Consortium, T. C. elegans S. (1998). Genome Sequence of the Nematode C . elegans : A Platform for Investigating Biology. *Science*, *282*(5396):2012–2018.

Cook, S. J., Jarrell, T. A., Brittin, C. A., Wang, Y., Bloniarz, A. E., Yakovlev, M. A., Nguyen, K. C. Q., Tang, L. T. H., Bayer, E. A., Duerr, J. S., Bülow, H. E., Hobert, O., Hall, D. H., & Emmons, S. W. (2019). Whole-animal connectomes of both Caenorhabditis elegans sexes. *Nature*, *571*(7763):63–71.

Corsi, A. K., Wightman, B., & Chalfie, M. (2015). A transparent window into biology: A primer on Caenorhabditis elegans. *Genetics*, *200*(2):387–407.

Cuentas-condori, A., & Miller, D. M. (2020). Synaptic remodeling , lessons from C . elegans. *Journal of Neurogenetics*, *0*(0):1–16.

Cuentas-Condori, A., Mulcahy, B., He, S., Palumbos, S., Zhen, M., & Miller, D. M. (2019). C. Elegans neurons have functional dendritic spines. *ELife*, *8*:1–24.

De Bono, M. (2003). Molecular approaches to aggregation behavior and social attachment. *Journal of Neurobiology*, *54*(1):78–92.

Doitsidou, M., Jarriault, S., & Poole, R. J. (2016). Next-generation sequencing-based approaches for mutation mapping and identification in Caenorhabditis elegans. *Genetics*, *204*(2):451–474.

El Fatimy, R., Davidovic, L., Tremblay, S., Jaglin, X., Dury, A., Robert, C., De Koninck, P., & Khandjian, E. W. (2016). Tracking the Fragile X Mental Retardation Protein in a Highly Ordered Neuronal RiboNucleoParticles Population: A Link between Stalled Polyribosomes and RNA Granules. *PLoS Genetics*, *12*(7):1–31.

Evans, T. (2006). Transformation and microinjection. *WormBook*, 1–15.

Fire, A. (1986). Integrative transformation of Caenorhabditis elegans . *The EMBO Journal*, *5*(10):2673–2680.

Formicola, N., Vijayakumar, J., & Besse, F. (2019). Neuronal ribonucleoprotein granules: Dynamic sensors of localized signals. *Traffic*, *20*(9):639–649.

Frøkjær-Jensen, C., Davis, M. W., Sarov, M., Taylor, J., Flibotte, S., LaBella, M., Pozniakovsky, A., Moerman, D. G., & Jorgensen, E. M. (2014). Random and targeted transgene insertion in Caenorhabditis elegans using a modified Mos1 transposon. *Nature Methods*, *11*(5):529–534.

Gendrel, M., Atlas, E. G., & Hobert, O. (2016). A cellular and regulatory map of the GABAergic nervous system of C. elegans. *ELife*, *5*:1–38.

Giandomenico, S. L., Alvarez-Castelao, B., & Schuman, E. M. (2021). Proteostatic regulation in neuronal compartments. *Trends in Neurosciences*, 1–12.

Gray, J. M., Karow, D. S., Lu, H., Chang, A. J., Chang, J. S., Ellis, R. E., Marietta, M. A., & Bargmann, C. I. (2004). Oxygen sensation and social feeding mediated by a C. elegans guanylate cyclase homologue. *Nature*, *430*(6997):317–322.

Hammarlund, M., & Jin, Y. (2014). Axon regeneration in C. elegans. *Current Opinion in Neurobiology*, *27*:199–207.

Hart, A. C. (2006). C. elegans Behavior. *WormBook*.

Hedgecock, E. M., Culotti, J. G., & Hall, D. H. (1990). The unc-5, unc-6, and unc-40 genes guide circumferential migrations of pioneer axons and mesodermal cells on the epidermis in C. elegans. *Neuron*, *4*(1):61–85.

Hekimi, S., Boutis, P., & Lakowski, B. (1995). Viable maternal-effect mutations that affect the development of the nematode Caenorhabditis elegans. *Genetics*, *141*:1351–1364.

Hobert, O. (2013). The neuronal genome of Caenorhabditis elegans. *WormBook: The Online Review of C. Elegans Biology*, 1–22.

Hobert, Oliver. (2010). Neurogenesis in the nematode Caenorhabditis elegans. *WormBook : The Online Review of C. Elegans Biology*, 1–24.

Jorgensen, E. M., & Mango, S. E. (2002). The art and design of genetic screens: Caenorhabditis elegans. *Nature Reviews Genetics*, *3*(5):356–369.

Kage-Nakadai, E., Kobuna, H., Funatsu, O., Otori, M., Gengyo-Ando, K., Yoshina, S., Hori, S., & Mitani, S. (2012). Single/low-copy integration of transgenes in Caenorhabditis elegans using an ultraviolet trimethylpsoralen method. *BMC Biotechnology*, *12*:1–9.

Kelly, W. G., & Fire, A. (1998). Chromatin silencing and the maintenance of a functional germline in Caenorhabditis elegans. *Development*, *125*(13):2451–2456.

Kohn, R. E., Duerr, J. S., McManus, J. R., Duke, A., Rakow, T. L., Maruyama, H., Moulder, G., Maruyama, I. N., Barstead, R. J., & Rand, J. B. (2000). Expression of multiple UNC-13 proteins in the Caenorhabditis elegans nervous system. *Molecular Biology of the Cell*, *11*(10):3441–3452.

Kutscher, L. M., & Shaham, S. (2014). Forward and reverse mutagenesis in C. elegans. *WormBook : The Online Review of C. Elegans Biology*, *212*:1–26.

Li, C., & Kim, K. (2008). Neuropeptides. *WormBook : The Online Review of C. Elegans Biology*, *212*:1–36.

Li, L., Yu, J., & Ji, S. J. (2021). Axonal mRNA localization and translation: local events with broad roles. *Cellular and Molecular Life Sciences*.

Li, Y., Camp, S., Rachinsky, T. L., Bongiorno, C., & Taylor, P. (1993). Promoter elements and transcriptional control of the mouse acetylcholinesterase gene. *Journal of Biological Chemistry*, *268*(5):3563–3572.

Liu, Q., Kidd, P. B., Dobosiewicz, M., & Bargmann, C. I. (2018). C. elegans AWA Olfactory Neurons Fire Calcium-Mediated All-or-None Action Potentials. *Cell*, *175*(1):57-70.

Mahoney, T. R., Luo, S., & Nonet, M. L. (2006). Analysis of synaptic transmission in Caenorhabditis elegans using an aldicarb-sensitivity assay. *Nature Protocols*, *1*(4):1772–1777.

Mclntire, S. L., Jorgensen, E., Kaplan, J., & Horvitz, H. R. (1993). The GABAergic nervous system of Caenorhabditis elegans. *Nature*, *364*(6435):337–341.

Mellem, J. E., Brockie, P. J., Madsen, D. M., & Maricq, A. V. (2008). Action potentials contribute to neuronal signaling in C. elegans. *Nature Neuroscience*, *11*(8):865–867.

Mello, C. C., Kramer, J. M., Stinchcomb, D., & Ambros, V. (1991). Efficient gene transfer in C.elegans: Extrachromosomal maintenance and integration of transforming sequences. *EMBO Journal*, *10*(12):3959–3970.

Mulcahy, B., Witvliet, D., Mitchell, J. K., Schalek, R., Berger, D., Wu, Y., Holmyard, D., Lu, Y., Ahamed, T., Samuel, A. D., Chisholm, A. D., Lichtman, J. W., & Zhen, M. (2022). Post-embryonic maturation of the C. elegans motor circuit. *BioRxiv*.

Nance, J., & Frøkjær-Jensen, C. (2019). The caenorhabditis elegans transgenic toolbox. *Genetics*, 212.

Nawa, M., & Matsuoka, M. (2012). The Method of the Body Bending Assay Using C. elegans. *Bio-Protocol*, *2*:1–2.

Oikonomou, G., & Shaham, S. (2011). The glia of Caenorhabditis elegans. *Glia*, *59*:1253–1263.

Pereira, L., Kratsios, P., Serrano-Saiz, E., Sheftel, H., Mayo, A. E., Hall, D. H., White, J. G., LeBoeuf, B., Garcia, L. R., Alon, U., & Hobert, O. (2015). A cellular and regulatory map of the cholinergic nervous system of C. Elegans. *ELife*, *4*:1–46.

Philbrook, A., Ramachandran, S., Lambert, C. M., Oliver, D., Florman, J., Alkema, M. J., Lemons, M., & Francis, M. M. (2018). Neurexin directs partner-specific synaptic connectivity in C. elegans. *ELife*, *7*:1–31.

Raizen, D. M., Zimmerman, J. E., Maycock, M. H., Ta, U. D., You, Y. J., Sundaram, M. V., & Pack, A. I. (2008). Lethargus is a Caenorhabditis elegans sleep-like state. *Nature*, *451*(7178):569–572.

Rajyaguru, P., & Parker, R. (2009). CGH-1 and the control of maternal mRNAs. *Trends in Cell Biology*, *19*(1):24–28.

Rand, J. B., & Russell, R. L. (1985). Properties and Partial Purification of Choline Acetyltransferase from the Nematode Caenorhabditis elegans. *Journal of Neurochemistry*, *44*(1):189–200.

Rapti, G. (2020). A perspective on C. elegans neurodevelopment: from early visionaries to a booming neuroscience research. *Journal of Neurogenetics*, *34*(3–4):259–272.

Ravanidis, S., Kattan, F. G., & Doxakis, E. (2018). Unraveling the pathways to neuronal homeostasis and disease: Mechanistic insights into the role of RNA-binding proteins and associated factors. *International Journal of Molecular Sciences*, *19*(8):1–49.

Sassa, T., Harada, S. I., Ogawa, H., Rand, J. B., Maruyama, I. N., & Hosono, R. (1999). Regulation of the UNC-18-Caenorhabditis elegans syntaxin complex by UNC- 13. *Journal of Neuroscience*, *19*(12):4772–4777.

Schuske, K., Beg, A. A., & Jorgensen, E. M. (2004). The GABA nervous system in C. elegans. *Trends in Neurosciences*, *27*(7):407–414.

Shaham, S. (2015). Glial development and function in the nervous system of Caenorhabditis elegans. *Cold Spring Harbor Perspectives in Biology*, *7*(4):1–14.

Singh, J. (2020). Harnessing the power of genetics : fast forward genetics in Caenorhabditis elegans. *Molecular Genetics and Genomics*, *296(1)*:1–20.

Sulston, J. E., Schierenberg, E., White, J. G., & Thomson, J. N. (1983). The embryonic cell lineage of the nematode Caenorhabditis elegans. *Developmental Biology*, *100*(1):64–119.

Takagi, S., Bénard, C., Pak, J., Livingstone, D., & Hekimi, S. (1997). Cellular and axonal migrations are misguided along both body axes in the maternal-effect mau-2 mutants of Caenorhabditis elegans. *Development*, *124*(24):5115–5126.

Touroutine, D., & Tanis, J. E. (2020). A Rapid, SuperSelective Method for Detection of Single Nucleotide Variants in Caenorhabditis elegans. *Genetics*, *216*(2):343–352.

Treinin, M., & Jin, Y. (2021). Cholinergic transmission in C. elegans: Functions, diversity, and maturation of ACh-activated ion channels. *Journal of Neurochemistry*, *158*(6):1274–1291.

White, J., Southgate, E., Thomson, J., & Brenner, S. (1986). The Structure of the Nervous System of the Nematode Caenorhabditis elegans. *The Royal Society*, 314.

Witvliet, D., Mulcahy, B., Mitchell, J., Meirovitch, Y., Berger, D., Wu, Y., Liu, Y., Koh, W. X., Parvathala, R., Holmyard, D., Schalek, R., Shavit, N., Chisholm, A., Lichtman, J., Samuel, A., & Zhen, M. (2020). *Connectomes across development reveal principles of brain maturation in C. elegans*. 1–26.

Yoshina, S., Suehiro, Y., Kage-Nakadai, E., & Mitani, S. (2016). Locus-specific integration of extrachromosomal transgenes in C. elegans with the CRISPR/Cas9 system. *Biochemistry and Biophysics Reports*, *5*:70–76.

Zhang, L., Ward, J. D., Cheng, Z., & Dernburg, A. F. (2015). The auxin-inducible degradation (AID) system enables versatile conditional protein depletion in C. elegans. *Development (Cambridge)*, *142*(24):4374–4384.